BeFo
STIFTELSEN BERGTEKNISK FORSKNING
ROCK ENGINEERING RESEARCH FOUNDATION

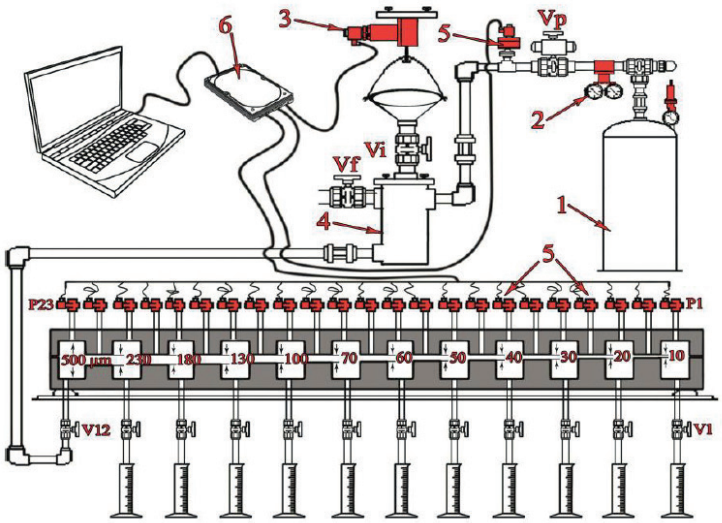

AN EXPERIMENTAL STUDY TO MEASURE GROUT PENETRABILITY, IMPROVE THE GROUT SPREAD, AND EVALUATE THE REAL TIME GROUTING CONTROL THEORY

Ali Nejad Ghafar
Almir Draganovic
Stefan Larsson

Cover figure: Schematic view of VALS: 1) gas container, 2) pressure regulator, 3) load cell, 4) grout tank, 5) pressure transducers, 6) DAQ

ROCK ENGINEERING RESEARCH FOUNDATION
STIFTELSEN BERGTEKNISK FORSKNING

AN EXPERIMENTAL STUDY TO MEASURE GROUT PENETRABILITY, IMPROVE THE GROUT SPREAD, AND EVALUATE THE REAL TIME GROUTING CONTROL THEORY

En experimentell studie för mätning av inträngningsförmåga av injekteringsmedel, förbättring av spridning av bruket, och utvärdering av RTGC-teorin

Ali Nejad Ghafar
Almir Draganovic
Stefan Larsson

BeFo Report 181
Stockholm 2024
ISSN 1104-1773
ISRN BEFO-R-181-SE

PREFACE

One of the major concerns in subsurface infrastructures is to provide the sealing required during both construction and operation. Ingress of water into such projects during the construction increases the time and costs. It is sometimes accompanied by environmental issues, e.g., lowering the groundwater tables, settlement of the structures, and destruction of vegetation. It can be hazardous to human life, e.g., falling icicles in tunnels in cold climate. It reduces the life cycle of the projects and increases the maintenance costs. To provide the sealing required, a governing parameter is to obtain sufficient spread of grout in surrounding fractures. This can be achieved using cement-based and/or chemical grouts. Despite satisfactory grout spread and sealing efficiency, use of chemical grout is prohibited in many countries due to hazardous environmental issues. Cement-based grout, which is cheaper with less environmental issues, is more common in grouting industry. However, in use of cement-based grout, filtration, which is a result of arching of the cement particles at a fracture constriction, restricts the grout spread. On this basis, this study is dedicated to investigate the grout penetrability/filtration properties in fractured hard rock.

The study was begun by a review of the existing methodologies developed to measure the grout penetrability. Then, a comparison was made between three of the most common used methods in Swedish grouting industry to provide a better understanding of filtration and to figure out which one is more reliable and why. Based on the achievements, a new test apparatus, so-called varying aperture long slot (VALS), was developed in the form of an artificial fracture with four-meter long and variable apertures of 230-10 μm. In the next step, an effort was conducted to improve the grout spread using low-frequency dynamic pressure impulses with different durations of peak/rest periods. The method, which was first tested using short slot, showed significant improvement on the amount of grout take. Dissipation of the pressure impulses was then examined along a much longer artificial fracture, VALS. Finally, due to the significance of optimization of grout spread in rock grouting, the real time grouting control (RTGC) theory, as one of the most common stop criteria in Swedish grouting industry, was examined in more realistic geometry condition using VALS with variable apertures. Even though the project was a limited study based on laboratory tests, the results were positive showing the potential of the methods that if could be further developed to full scale field operations, might influence on grouting industry significantly.

This report is a summary of a doctoral study that was carried out by Ali Nejad Ghafar during 2013-2017 at the Division of Soil and Rock Mechanics, Department of Civil and Architectural Engineering, Royal Institute of Technology (KTH). The research was supervised by Prof. Stefan Larsson (Main supervisor) Dr. Amir Draganovic (Co-supervisor), and Prof. Emeritus Håkan Stille (Expert support). The project had support from a reference group with the following participants: Håkan Stille (KTH), Daniel Eklund (SKB), Tommy Ellison (Besab), Robert Sturk (Skanska), Thomas Janson (Tyréns), Emmeli Johansson (SKB), Niclas Bockgård (Golder) and Per Tengborg (BeFo).

The project was financed by the Rock Engineering Research Foundation (BeFo), the Swedish Transport Administration, and the Development Fund of the Swedish Construction Industry (SBUF).

Stockholm
Per Tengborg

FÖRORD

Ett av de största problemen i infrastruktur för undermarkskonstruktioner är att uppnå den tätning som krävs under både bygg- och drifttid. Vatteninflöde under byggtiden av sådana projekt kan öka tiden och kostnaderna. Det kan medföljas ibland också av miljöfrågor, till exempel sänkning av grundvatten, sättningar och förstöring av vegetation. Det kan vara också farligt för människoliv, t ex fallande istappar i tunnlar i kallt klimat. Vatteninflödet minskar också projektets livscykel och ökar underhållskostnaderna. För att åstadkomma den tätning som krävs måste en tillräcklig spridning av injekteringsbruket i omgivande bergssprickor erhållas. Det kan uppnås genom användning av cementbaserade och/eller kemiska bruk. Trots tillfredsställande bruksspridning och tätningseffektivitet är användning av kemiskt bruk förbjuden i många länder på grund av miljöpåverkan. Cementbaserat bruk är billigare och har en mindre miljöpåverkan och är mycket vanligare inom byggindustrin. Men vid användning av cementbaserat bruk begränsar filtreringen spridning av bruket. Filtreringen är ett resultat av partikelansamlingen vid liten sprickvidd. Baserat på detta problem är denna studie avsedd för att undersöka inträngningsförmåga och filtreringsegenskaper av bruket i sprickigt berg.

Studien inledes genom en översyn av de befintliga metoder som utvecklats för att mäta inträngningsförmågan hos bruket. Därefter gjordes en jämförelse mellan tre av de vanligaste metoderna i svensk byggindustri för att ge en bättre förståelse av filtrering och för att ta reda på vilken metod är mer tillförlitlig och varför. Baserat på dessa studier utvecklades en ny testapparat, en 4 m lång spalt med varierande spaltvidder mellan 230-10 μm (VALS). I nästa steg avsågs att förbättra inträngning av bruket med hjälp av lågfrekventa dynamiska tryckimpulser med olika långa topp och viloperioder. Metoden, som först testades med användning av kort spalt, visade signifikant förbättring av mängden av injekterad bruk. Minskning av tryckimpulserna undersöktes sedan längs den 4 m långa spalten (VALS). Slutligen undersöktes RTGC-teorin i laboratoriet med VALS. RTGC är det senaste utvecklade metoden som används i Sverige vid injektering med syfte att optimera bruksspridning i bergssprickor. Trots att projektet var en begränsad laboratoriestudie, var resultaten positiva och visade potentialen hos metoden. Testmetoden skulle kunna utvecklas vidare till fullskaliga fältmätningar och detta skulle kunna påverka industrin betydligt.

Rapporten är en sammanfattning av en doktorandstudie som utfördes av Ali Nejad Ghafar under 2013–2017 vid Avdelningen för Jord- och bergmekanik, Institutionen för Byggvetenskap, KTH. Forskningen handledes av professor Stefan Larsson som huvudhandledare, Dr Amir Draganovic som biträdande handledare och professor emeritus Håkan Stille som expertstöd. Projektet fick stöd av en referensgrupp som bestod av Håkan Stille (KTH), Daniel Eklund (SKB), Tommy Ellison (Besab), Robert Sturk (Skanska), Thomas Janson (Tyréns), Emmeli Johansson (SKB), Niclas Bockgård (Golder) och Per Tengborg (BeFo).

Projektet finansierades av Stiftelsen Bergteknisk Forskning (BeFo), Trafikverket och SBUF.

Stockholm
Per Tengborg

SUMMARY

To provide the sealing required in subsurface infrastructures, obtaining sufficient spread in grouting operations is essential. Cement-based grouts are the most common materials used in the grouting industry due to several advantages, especially from an economic and environmental point of view. However, the penetrability properties of the grout used influence the corresponding spread significantly. The main objectives in this investigation were therefore to study: a) which of the existing methodologies developed to measure grout penetrability are more reliable?; b) how can grout penetrability be measured more realistically?; c) how can the grout spread be improved effectively using dynamic pressure impulses?; and d) is it feasible to apply real time grouting control (RTGC) theory to predict the grout spread in an artificial fracture with variable aperture?

Accordingly, in Part (a) of the study, a review was first conducted on all existing methodologies developed to measure grout penetrability. A comparison was made between Filter-pump and Penetrability-meter (i.e. two of the most frequently used methods in the Swedish grouting industry) and Short slot under as similar test conditions as possible. The study decisively considered Short slot more reliable due to its more realistic test conditions (i.e. the geometry, pressure, and grout volume) and an accurate evaluation method.

In part (b), the so-called varying aperture long slot (VALS), a four-meter long artificial fracture with variable apertures of 230-10 μm, was developed as a more realistic method to study the penetrability properties of any grout at static/dynamic pressure conditions up to 20 bar.

In part (c), a low-frequency rectangular pressure impulse was introduced to improve the grout spread effectively by successive erosion of the produced filter cakes at a fracture constriction in consecutive cycles. The results showed up to 11 times improvement in the volume of grout-take in experiments using Short slot with 30-43 μm constrictions. The extent of the dissipation of the pressure impulses along a fracture was then investigated using VALS. The results revealed that remaining amplitudes of the pressure impulses after 2.0 and 2.7 m (with aperture ranges of 230-70 and 230-50 μm) can be as large as 46% and 25% of the initial/applied amplitude, respectively, to influence the grout spread.

In part (d), to investigate the performance of the RTGC theory in a fracture with variable aperture, VALS was once again introduced. The study showed a relatively satisfactory agreement between the experimental results and the predictions of the grout propagation using the hydraulic aperture of VALS, whereas the predictions using the mean physical aperture showed considerably faster spread. This suggested that use of the mean physical aperture does not always give a good approximation of the fracture apertures to employ in predictions using the RTGC theory, as is mainly used nowadays in the grouting industry. Depending on the geometry conditions, use of hydraulic aperture might provide a more realistic prediction of the grout spread.

KEYWORDS

Cement-based grout, Penetrability, Filtration, Varying Aperture Long Slot-VALS, Dynamic grouting, RTGC theory

SAMMANFATTNING

För att uppnå den täthet som krävs i undermarkskonstruktioner är det nödvändigt att uppnå tillräcklig spridning av bruket vid injekteringen. Cementbaserade injekteringsmedel är vanligast inom injekteringsindustrin, eftersom det har flera fördelar, särskilt från ekonomisk och miljömässig synvinkel. Eftersom inträngningsförmågan kan påverkas betydligt hos injekteringsmedel beroende på vilket bruk man använder, är syftet med denna avhandling att studera: a) Vilka av de befintliga metoder som har utvecklats för att mäta injekteringsmedels inträngningsförmåga är tillförlitliga? b) Hur kan man mäta inträngningsförmågan hos injekteringsmedel mer realistiskt? c) Hur kan man förbättra spridningen hos injekteringsmedel med hjälp av dynamiska tryckimpulser? och d) Kan Real Time Grouting Control (RTGC)-teorin användas för att förutse spridningen hos injekteringsmedel i en artificiell spricka med varierande vidd?

I del a) av studien genomfördes en undersökning av alla befintliga metoder som har utvecklats för att mäta inträngningsförmågan hos injekteringsmedel. Därefter genomfördes en jämförelse mellan Filterpumpen, Filterpressen (d.v.s. två av de vanligaste metoderna i svensk injekteringsindustri) och metoden Kort spalt under så lika provförhållanden som möjligt. Studien visade att Kort spalt är tillförlitligare på grund av dess mer realistiska provförhållanden (d.v.s. geometrin, trycket och injekteringsvolymen) och är därmed en bättre utvärderingsmetod.

I del b) utvecklades en så kallad Varying Aperture Long Slot (VALS), en fyra meter lång artificiell spricka med minskande spaltvidder (från 230 till 10 μm), som är en mer realistisk metod för att studera inträngningsförmågan hos injekteringsmedel under statiska/dynamiska tryckförhållanden upp till 20 bar.

I del c) användes en lågfrekvent rektangulär tryckimpuls för att förbättra spridningen hos injekteringsmedlet. Det utfördes genom en successiv erosion under påföljande cykler av de filterkakor som har byggts vid förträngningar. Resultaten visade en förbättring på upp till 11 gånger mer volym i mätningar med Kort spalt med 30–43 μm breda spaltvidder. Spridningen av tryckimpulserna undersöktes därefter längs VALS. Resultaten visade att de bibehållna amplituderna av tryckimpulser kan vara så stora som 46% respektive 25% av den applicerade amplituden på avståndet 2,0 m respektive 2,7 m in i sprickan.

I del d) användes VALS igen för att undersöka om RTGC-teorin kan användas för att bedöma spridningen av injekteringsmedel i en konstgjord spricka med variabel spaltvidd. Studien visade en förhållandevis tillfredsställande överensstämmelse mellan försöksresultaten och förutsägelserna av spridningen hos injekteringsmedel när man tog hänsyn till den hydrauliska öppningen. Som jämförelse gav förutsägelserna baserade på den genomsnittliga fysiska öppningen (felaktigt) en betydligt snabbare spridning. Detta visar att användning av den genomsnittliga fysiska öppningen inte alltid är lämpligt vid tillämpning av RTGC-teori. Beroende på de geometriska förhållandena kan den hydrauliska öppningen ge en mer realistisk förutsägelse av spridningen hos injekteringsmedlet.

NYCKELORD

Cementbaserat injekteringsmedel, Inträngningsförmåga, Filtration, Varying Aperture Long Slot-VALS, Dynamisk injektering, RTGC-teorin

TABLE OF CONTENTS

1. INTRODUCTION

To obtain the required sealing in any underground facility in rock, various parameters are involved. Among the governing parameters, sufficient grout spread, i.e. obtaining adequate penetration length during the grouting operation is of the utmost importance (Houlsby 1990; Lombardi 2003; Warner 2004; Gustafson and Stille 2005; Fransson 2008; Gustafson et al. 2013; Stille 2015). To obtain sufficient grout spread, various kinds of grouting materials, generally categorized as a) cement-based grouts and b) chemical grouts, have been employed by the grouting industry worldwide (Houlsby 1990; Karol 2003; Warner 2004). Despite the satisfactory grout spread and considerable sealing efficiency, chemical grouts have sometimes shown severely hazardous environmental issues, which has made their use considerably limited in most countries (Weideborg et al. 2001). Cement-based grouts, which are cheaper and cause less environmental issues, are though mostly preferred and considered a more reliable alternative. However, in application of cement-based grouts, the filtration tendency of the cement particles is a matter of controversy. The filtration, which occurs due to the arching/bridging of the cement particles at a fracture constriction, restricts the grout spread (Eriksson et al. 2000; Eriksson and Stille 2003; Draganovic and Stille 2011). In addition, the grout's rheological properties, i.e. the viscosity and the yield stress, are the other governing parameters that control the grout spread (Håkansson 1993; Schwarz 1997; Eriksson et al. 2004; Eklund 2005; Banfill 2006; Eklund and Stille 2008; Rafi 2013; Mohammed et al. 2014). Several researchers have therefore devoted a great deal of time and effort to realize different aspects of the grout properties as a fundamental means to improve the grout spread. On this basis, this investigation is also dedicated to studying the grout penetrability properties in fractured hard rock.

Several test apparatus and evaluation methods have been developed over the years to determine the penetrability and filtration tendency of cement-based grout in both the lab and the field. The diversity and disagreement over the results obtained, however, indicate that those methods might not satisfactorily replicate the filtration at a fracture constriction as occurs in grouting operations in fractured hard rock (Draganovic and Stille 2011, 2014; Ghafar et al. 2017a). That would probably be due to the inherent deficiency in their design being based on diverse and occasionally unrealistic assumptions, limitations, and test conditions (Ghafar et al. 2017a). Our concern is therefore of the existing test methodologies developed to measure grout penetrability, which one is more reliable and how?

In addition, to determine grout penetrability in fractured hard rock, no realistic standard has yet been established. The existing methods are each associated with certain advantages and drawbacks, which make the results obtained difficult to relate to grouting in rock fractures. This suggests the need for a better test methodology to evaluate grout penetrability in fractured hard rock that replicates the filtration at a fracture constriction more realistically.

Comparing the results of the existing methodologies developed to measure grout penetrability reveals that one of the factors governing the filtration and consequently the grout spread is the applied pressure. A sufficient increase in the applied pressure decreases the filtration tendency and improves the grout spread by increasing the potential for erosion of the unstable filter cakes produced at a fracture constriction (Eriksson et al. 1999; Hjertström 2001; Draganovic and Stille 2011, 2014; Stille et al. 2012). Nobuto et al. (2008) showed that a

stepwise pressure increment decreases the potential for clogging of the cement particles at the entrance of a fracture. Pusch et al. (1985) were probably the first to demonstrate the influence of high-frequency oscillating pressure on improving the grout spread. Borgesson and Jansson (1990) further examined a high-frequency large-amplitude oscillating pressure superimposed on an underlying pressure of 20 bar and illustrated that even a low water content cement grout can penetrate well through 100 μm artificial fractures. The latter described the corresponding mechanism of action as a reduction in grout viscosity due to the applied high-frequency oscillation, whereby the grout's internal structure was disrupted and reorganized to provide a lower viscosity suspension. Wakita et al. (2003) also investigated the same method using oscillating amplitudes of up to 5 bar superimposed on an underlying pressure of 10 bar and in similar fashion to the previous investigations obtained an increase in the flow rate and the total volume of grout take. Mohammed et al. (2015) further elaborated on the method and once again recognized it as a potential solution to improve the grout spread. Besides those promising results, the method has, however, not yet been industrialized due to the limited efficiency and quick dissipation of the high-frequency oscillation along a fracture. To address these issues and employ the method to improve the grout spread in rock fractures effectively, the solution might be the use of a different shape and frequency of the applied pressure that indeed requires further investigation.

The necessity for sufficient grout spread is more discernible in the grouting operations in subsurface infrastructures with higher sealing demands, such as in nuclear/toxic waste repositories, which has become one of the major concerns in Scandinavia and especially in Sweden (Pusch et al. 2012). Accordingly, one of the main issues is insufficient grout spread within the fracture network surrounding the facility. This deteriorates the obtained sealing and the resulting durability significantly. On the other hand, the unnecessary spread of grout beyond the required penetration length in rock fractures is uneconomic and in some cases has also been accompanied by severe environmental issues. Optimization of grout spread is therefore of the greatest concern in rock grouting to provide a reliable and simultaneously an economic tight zone around the facility. Several stop criteria have therefore been developed to monitor and control the grout spread, from which the real time grouting control (RTGC) theory has received a lot of attention in the Swedish grouting industry. The theory predicts the extent of the grout spread over time in rock fractures using the grout's rheological properties and the applied pressure (Gustafson and Stille 1996, 2005; Kobayashi et al. 2008; Axelsson et al. 2009; Tsuji et al. 2012; Stille et al. 2012; Gustafson et al. 2013; Stille 2015). It has been developed based on several fundamental assumptions, from which the uniform fracture aperture is probably the most significant. Accordingly, all the laboratory efforts, the aim of which was to investigate the performance of the RTGC theory, have been conducted in either pipes (Håkansson 1993) or parallel plates with constant apertures (Gustafson et al. 2013). This means that the theory has not yet been sufficiently investigated in the lab with the presence of constrictions and varying apertures similar to the geometry of a real fracture in rock.

1.1 Objectives and scope of work

The main objectives of this study were therefore to answer the following questions:

a) Which of the existing test methodologies developed to measure grout penetrability are more reliable and how?

b) How can grout penetrability be measured more realistically?

c) How can the grout spread be improved effectively using dynamic pressure impulses?

d) Is it feasible to employ the RTGC theory to predict the grout spread in an artificial fracture with variable aperture?

Accordingly, the report comprises four complementary parts as follows:

Part (a) is dedicated to a brief review of all existing methods developed to measure grout penetrability. Filter pump and Penetrability meter, two of the most frequently used methods in the Swedish grouting industry, were therefore selected for comparison due to their simplicity and applicability in both the lab and the field. Short slot, with more realistic test conditions and a more accurate evaluation method, was chosen as the basis for this comparison even though it was only applicable in the lab. To make the analogy reasonable, the test apparatus and the test procedure in both Filter pump and Penetrability meter were modified to operate under as similar test conditions as possible to those in Short slot. The aim was to understand the nature of the grout penetrability to better evaluate the reliability and functionality of the instruments, and finally yet importantly figure out how to measure grout penetrability more realistically.

In part (b), the objective was to contribute to an improved test methodology to study the grout penetrability properties in fractured hard rock. Accordingly, a more realistic experimental apparatus, the so-called varying aperture long slot (VALS), was developed. The idea was to replicate the grouting operation and the filtration through the rock fractures using an artificial fracture with 4 m long and variable apertures of 10-230 μm. The test apparatus was applicable to examine grouts of any kind at both static and dynamic pressure conditions up to 20 bar. It was also able to monitor the injected grout weight and the grout's internal pressure before and after each constriction as a function of time.

In part (c), a low-frequency rectangular pressure impulse was introduced as a new alternative to improve the grout spread. The idea was to better control the filtration by successive erosion of the produced filter cakes at a fracture constriction in consecutive cycles. Two compositions of the peak/rest periods (i.e. 4 s/8 s and 2 s/2 s) were examined using Short slot with 30-43 μm constrictions. The aim was to investigate the influence of the new shape and frequency of the applied pressure on the grout spread within micro-fractures narrower than 70 μm. Afterwards, to investigate the dissipation of the pressure impulses along a fracture, VALS was once again introduced. The goal was to determine the remaining amplitudes of the impulses after 2.0 and 2.7 m (with aperture ranges of 70-230 and 50-230 μm) and to monitor the associated filtration and erosion at the applied pressure with 2 s/2 s peak/rest periods and a maximum of 15 bar.

Finally, part (d) was a novel effort to examine the performance of the RTGC theory to predict the grout spread in an artificial fracture with variable aperture. Hence, VALS was once again assigned for the investigation. The set-up provided the opportunity to examine the theory for grout flow between two parallel plates only in one-dimensional flow condition, but with sections having variable apertures of 10-230 μm, which were anticipated to be more similar to a real fracture in rock. The study was conducted based on a comparison between the experimental results and the analytical predictions of the grout propagation over time. The

predictions were carried out using the hydraulic and the mean physical apertures of VALS at the applied pressure of 15 bar.

1.2 Limitations

Some of the limitations associated with this study can be summarized as follows:

1.2.1 Number of test repetitions

The first issue that might be considered as a limitation in the current investigation is the number of experiments conducted in each part of the study. However, depending on the sensitivity of each part and based on our engineering judgement, the number of tests performed was considered to be sufficient for drawing the corresponding conclusions.

1.2.2 Geometry

Even though the geometries of Short slot and VALS employed in this study were considered to be more realistic than the other existing methodologies, several issues still remain unsolved. For instance, the limited numbers of constrictions in Short slot and VALS are probably far from the frequency of the irregularities that might exist in a real fracture in rock. The sharp/instantaneous variation of the apertures in both test apparatus is the other influential factor that might be different compared to what exists in a real fracture in rock. The surface roughness of the parallel steel plates, the distance between the constrictions, and the distribution of the apertures might also be rather different from what exists in reality. In addition, due to their specific design and geometry, both methods are only applicable to study the grout flow in 1D (one-dimensional) flow conditions. These limitations should be taken into consideration when drawing conclusions and especially when planning for the future steps of the project.

1.2.3 Technical

In part (c) of the investigation, in order to verify the proposed mechanism of improvement of grout penetrability under application of rectangular pressure impulse, it was necessary to observe the pattern of the grout flow passing through the constriction in Short slot. In parts (b) and (c), to study the filtration and erosion mechanisms at each constriction and determine their potential influences on grout spread, it was necessary to observe the grout flow through VALS. Finally, in part (d), in order to examine the ability of the RTGC theory to predict the grout propagation in comparison with the experimental results, tracking the grout front along VALS was required. Hence, the use of transparent materials, e.g. Plexiglas or Polycarbonate sheets in the production of VALS could be a proper choice. However, this was found to be impossible due to the limited bending capacity of the transparent sheets to withstand 15 bar pressure. Therefore, to fulfil the required strength properties, stainless steel was considered the best option to produce VALS. To solve this issue in future steps of the project, an indirect solution might be the use of Computational Fluid Dynamics (CFD) to simulate the grout flow in VALS at various test conditions.

1.3 Organization of the report

After presenting an introduction to motivate this investigation, the objectives, the scope of work, and finally some of the limitations associated with the study are discussed in chapter 1. The four fundamental questions, presented as the objectives of the study, provide the bases of the following four chapters. Chapter 2 is dedicated to a review of all the existing test

methodologies developed to measure grout penetrability. This is followed by a comparison between Filter pump, Penetrability meter, and Short slot with the focus on their limitations and deficiencies. Chapter 3 presents the development of a more realistic experimental apparatus, the so-called varying aperture long slot (VALS), to study the grout penetrability properties in fractured hard rock. The instrument has been designed based on the benefits and drawbacks of the existing methods recognized in Chapter 2. In chapter 4, a low-frequency rectangular pressure impulse is introduced as a new alternative of using the applied pressure to improve the grout spread. To investigate the efficiency of the method, Short slot with 30 and 43 μm apertures were employed. Thereafter, to study the dissipation of the pressure impulses and the corresponding filtration and erosion, VALS was once again employed. Chapter 5 represents a novel effort to investigate the performance of the RTGC theory with the presence of constrictions in VALS. Planned future work and recommended projects are then presented in chapter 6. Finally, references are listed in chapter 7.

2. Measurement of grout penetrability - Part (a)

Due to the significance of the grouting operations and the complexity involved, several researchers have dedicated much of their lives to investigating grouting from different perspectives. Various test instruments/methods have therefore been developed over the years to recognize and measure different aspects of grout penetrability. However, according to the literature, their obtained results have occasionally been contradictory. This is principally because those instruments/methods have been developed based on different assumptions, limitations, and test conditions. Therefore, part (a) of this investigation is dedicated to studying all the existing methodologies in detail to determine their negative and positive features.

2.1 Existing methodologies

2.1.1 Sand column

Sand column is a common method for measuring grout penetrability as detailed in French standard (NF P 18-891). The method was used in several investigations conducted by Bergman (1970), Schwarz (1997), Zebovitz et al. (1989), Paillere et al. 1989, Atkinson and Schuller (1993), Andreou et al. (2008), Axelsson et al. (2009), and Miltiadou-Fezans and Tassios (2012) among others. A general depiction of the test set-up according to Axelsson et al. (2009) is illustrated in Fig. 1. In order to start an experiment with Sand column, the pressurized grout in the grout container is pushed out towards a transparent tube filled with sand of a predefined particle size distribution. Sand column is normally used to evaluate grout penetrability using three different approaches: 1) measurement of the water height in the water column in the saturated condition, 2) measurement of the total volume of the injected grout in the unsaturated condition, and 3) visual inspection of the penetrated grout through the sand column.

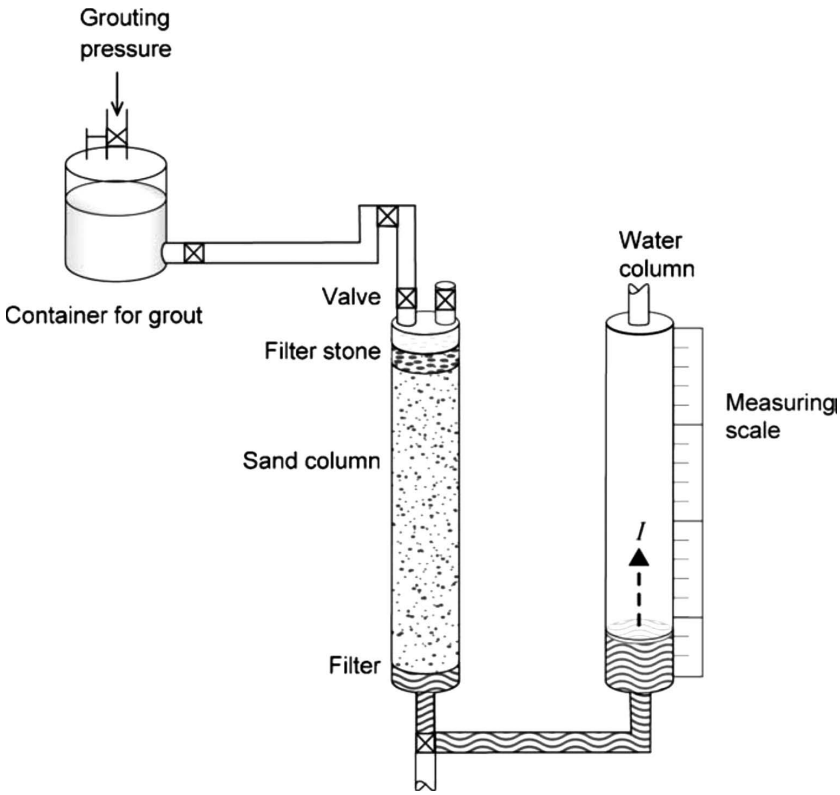

Fig. 1 Schematic view of Sand column according to Axelsson et al. (2009)

Due to considerable difference between the flow pattern in a porous medium and slot geometry, several investigations have aimed to correlate the results of the penetrability obtained from Sand column to a real fracture in rock (Bergman 1970; Gustafson and Stille 1996; Schwarz 1997; Gustafson and Stille 2005; Axelsson and Gustafson 2007; Draganovic 2009; Axelsson et al. 2009). Eventually, Axelsson et al. (2009) presented a fairly complete interpretation of the filtration mechanism in a porous medium. The latter categorized the corresponding filtration mechanism into: a) clogging (i.e. the cement grains stick together before entering an opening), b) filtration (i.e. the cement grains enter the opening but gradually separate from the flow and finally plug the pores), and c) resistance (i.e. the grout pressure is overcome by the frictional resistance in the opening's walls). Obtaining a rational relationship between the grout penetrability in those two media, however, was found to be quite difficult or impossible.

2.1.2 Pressure chamber or Filter press

Pressure chamber or Filter press is another method developed by Gandais and Delmas (1987) to measure the filtration stability of cement-based grout. In this method, the grout is pressurized in the grout container by compressed air to penetrate through a filtering medium with known penetrability made of paper, fine sand, soft rock, etc. A general depiction of the method as seen in Widmann (1996) is shown in Fig. 2.

According to Gandais and Delmas (1987), the density of the filter cake produced at the surface of the filtering medium varies linearly with depth. It is also proportional to the volume of the water passed through the filter. They considered the filtration mechanism in Pressure chamber to be representative of what occurs through a real fracture in rock. The grout under pressure is pressed against the fracture walls. Due to the porosity of the rock matrix and the existing micro-cracks, the grout is filtered through the walls. Eventually, the flow stops due to the plug formation of the cement particles and clusters, as shown in Fig. 3. According to Draganovic (2009), this filtration mechanism is, however, irrelevant in rock fractures.

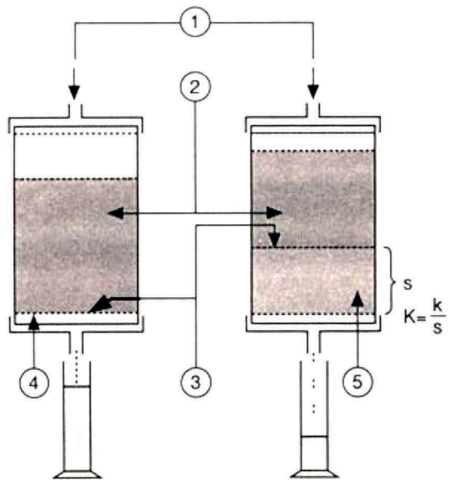

Fig. 2 Schematic view of Pressure chamber as seen in Widmann (1996)

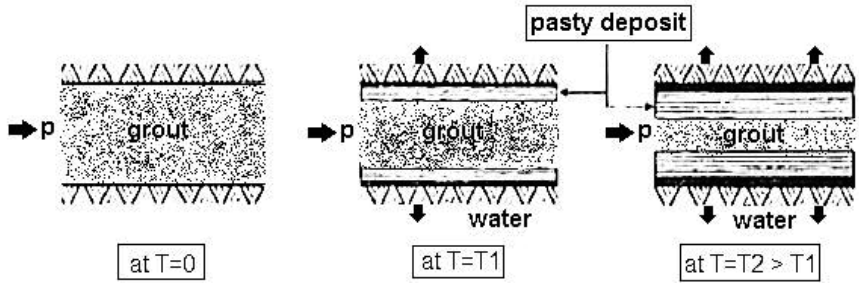

Fig. 3 Plug formation as depicted in Gandais and Delmas (1987)

2.1.3 Filter pump

Filter pump, developed by Hansson (1995), is another method designed to evaluate the filtration stability of cement-based grout. It is a common used method in the Swedish grouting industry, especially for quality control of cement due to the simplicity of its application in both lab and field. A general depiction of the method as seen in Hansson (1995) is shown in Fig.4. In order to start an experiment, the instrument's handle is pulled out to suck the grout mix into the instrument's tube through a woven metal mesh filter with various openings of 32, 45, 75, 100, and 125 μm in consecutive tests, respectively (Hansson 1995). The total grout volume passed through each filter is then plotted against the corresponding filter width to provide a qualitative evaluation of the grout filtration stability (Eriksson et al. 2000). To analyze the obtained graph, they suggested two parameters, b_{min} and b_{crit}, as shown in Fig. 5. In the figure, the maximum filter width associated with only negligible passed grout represents the value of b_{min}, whereas the minimum filter width with the maximum volume of the passed grout (300 ml) represents the value of b_{crit}. As defined by Eriksson and Stille (2003), b_{min} is the minimum fracture aperture that a specific grout can penetrate at all and b_{crit} is the minimum fracture aperture that a specific grout can penetrate without filtration. At the apertures between these values, the grout is partially filtered, whereas no grout can penetrate through an aperture smaller than b_{min}. These properties are considered to be the fundamentals in evaluation of grout penetrability in the current investigation.

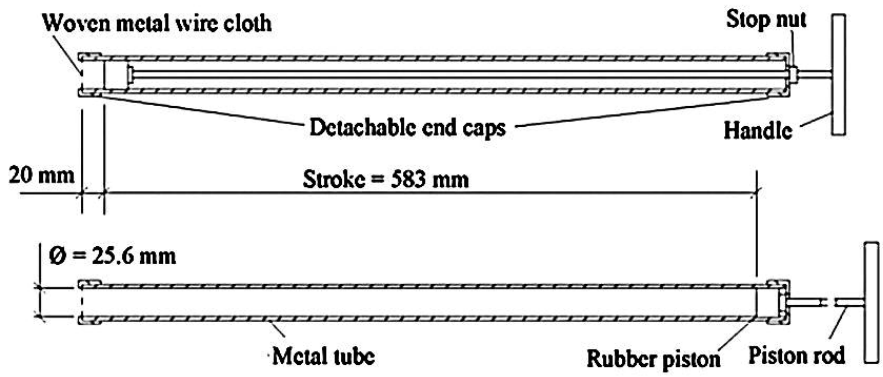

Fig. 4 Schematic view of Filter pump as seen in Hansson (1995)

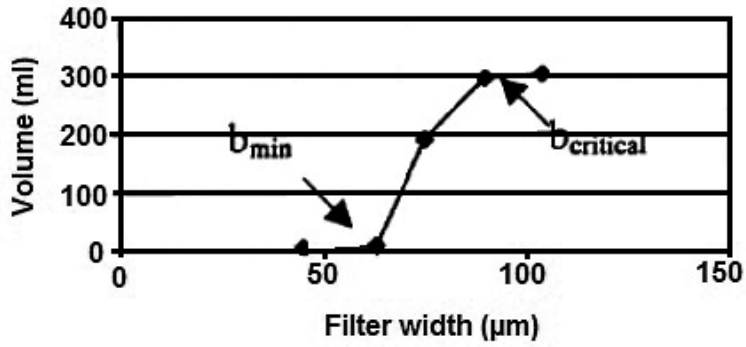

Fig. 5 Evaluation of b_{min} and b_{crit} according to Eriksson et al. (2000)

2.1.4 Penetrability meter

Penetrability meter, developed by Eriksson and Stille (2003), is the next method designed to measure grout penetrability (Fig. 6). It is commonly used in the Swedish grouting industry, once again since it is simple to apply in both lab and field. The method comprises a grout container linked to an air pressure pump on top and an outlet valve at the bottom that is connected to a tubular filter holder. In order to start an experiment, the pressurized grout (at one bar pressure) is pushed out through the woven metal mesh filters with various openings in consecutive tests as described earlier under Filter pump. In this method, grout penetrability is evaluated using the same methodology and parameters, i.e. the values of b_{min} and b_{crit} as defined under Filter pump, except that b_{crit} is measured for 1 l of the passed grout.

Penetrability meter was further employed by Eklund and Stille (2008) to investigate the difference between the influences of the mesh and the slot geometries. They concluded that the probability of the filtration in the mesh geometry, where the arching occurs from four sides, is higher than that in the slot geometry, where the filtration occurs from only two sides. It should, however, be borne in mind that the filtration mechanism in the slot geometry is more similar to what occurs in a real fracture in rock (Fig. 7).

Fig. 6 Penetrability meter developed by Eriksson and Stille (2003)

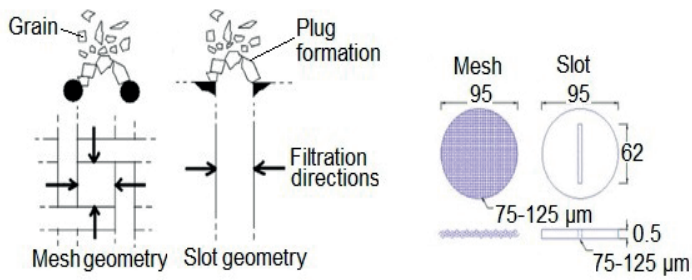

Fig. 7 Mesh and slot geometries in penetrability meter (Eklund and Stille, 2008)

2.1.5 NES and Nobuto methods

The NES method, developed by Sandberg (1997), is probably the oldest method designed to measure grout penetrability using slot geometry. A general depiction of the method as seen in Sandberg (1997) is shown in Fig. 8. It comprised an artificial fracture in the form of two parallel steel plates that are connected to the bottom of a grout tank (Fig. 8). The grout tank itself was suspended from a digital scale to monitor the grout's weight over time. The applied pressure was normally provided by a high-pressure gas tank attached to the system on top. In each experiment, the pressurized grout (at pressures ≤ 20 bar) was pushed out through the aperture between the parallel plates (with known geometries). The method was later used to evaluate the grout's filtration tendency based on the values of b_{min} and b_{crit} as defined by Eriksson et al. (2000).

A modified version of the method was later employed by Nobuto et al. (2008), using the field mixing, agitation, and injection equipment that could operate at pressures ≤ 50 bar. Using a stepwise pressure increment, they illustrated a significant improvement in grout penetrability with the mechanism of action shown in Fig. 9. In this figure, the flow eventually stops due to the arching/bridging of the cement particles at the entrance of the channels.

Stepwise increases in pressure, however, cause the unstable arches to collapse and the channels once again become open for further grout flow, resulting in a considerable improvement in grout penetrability.

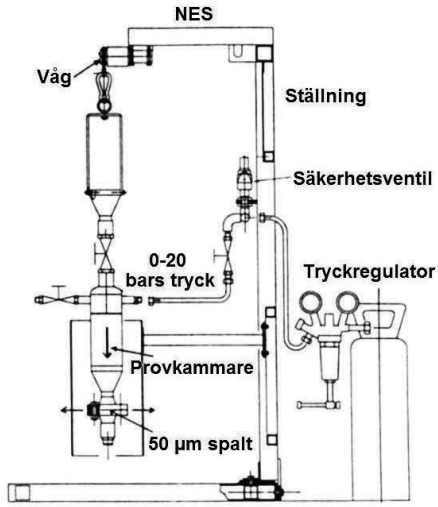

Fig. 8 Schematic view of NES method (Sandberg, 1997)

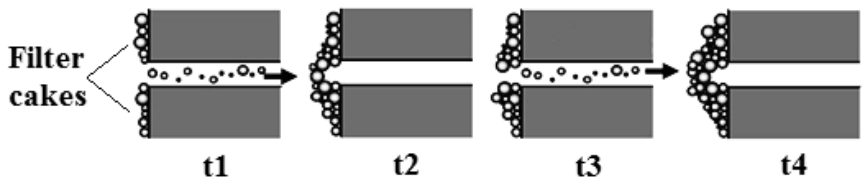

Fig. 9 Filtration process suggested by Nobuto et al. (2008)

2.1.6 PenetraCone

PenetraCone, developed by Axelsson and Gustafson (2010), provided another alternative to measure grout penetrability in both lab and field. The method comprised two conical cylinders, i.e. the outer and inner cones, with an aperture in-between that could be adjusted by rotating the inner one (Fig. 10). In this method, every test normally began using a proper large aperture that allowed a steady grout flow. This initial aperture was gradually decreased by the operator to change the undisturbed grout flow to drip. The aperture was then returned to its initial size to again provide a steady grout flow. In the second round, the initial aperture was once again gradually reduced to reach the flow stop. As defined by Axelsson and Gustafson (2010), using a PenetraCone, b_{filter} was the aperture size when the continuous grout flow turned to drip and b_{stop} was the aperture size at the flow stop.

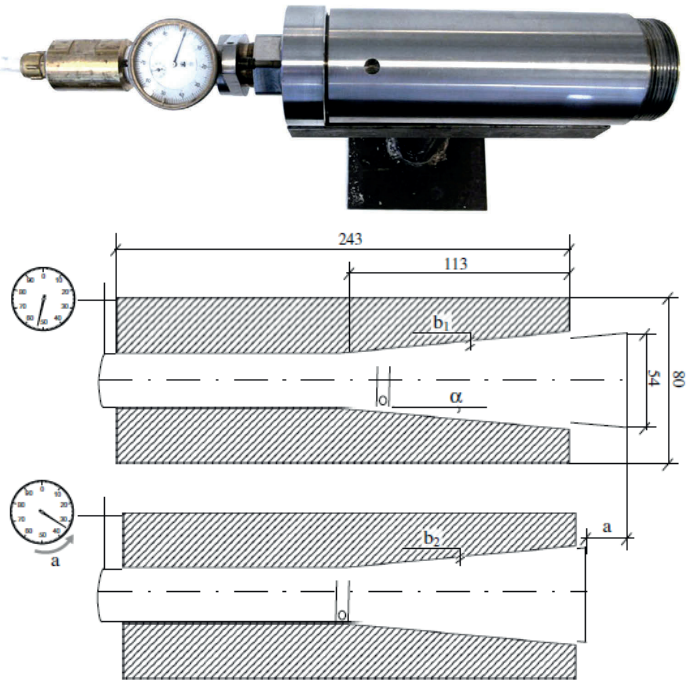

Fig. 10 PenetraCone seen in Axelsson et al. (2009)

2.1.7 Short Slot

Short slot is another test method, developed by Draganovic and Stille (2011), to measure the penetrability properties of cement-based grout. The method comprised two parallel steel plates in the form of a slot (i.e. an artificial fracture) with two flow channels, each having one constriction of the same size. The method operated based on a set-up similar to that in the NES method. The slot itself was attached to the bottom of a grout tank with 2.6 l capacity that was suspended from a digital scale to register the grout's weight over time. The applied pressure (≤ 20 bar) was normally provided using a high-pressure gas tank. To replicate the filtration process in fractures with various apertures, several slots with various constrictions (300-30 µm) were available. The main difference between Short slot and NES methods was the existence of constrictions in Short slot. Accordingly, the filtration in Short slot appeared at the constrictions, and in the NES method at the connection between the "borehole" and the slot (i.e. at the entrance of the slot). In this method, a linear relationship in weight-time measurement was an indication of no filtration. However, a non-linear relationship was representative of filtration. Figure 11 shows cross-sections of the constriction and the arching/bridging mechanism of the cement particles discussed in detail by Draganovic and Stille (2011).

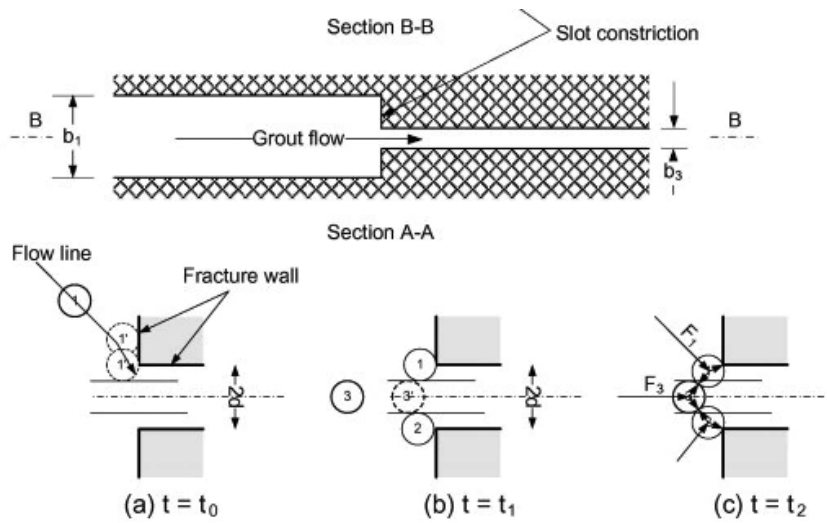

Fig. 11 Cross-section of Short slot (upper) and arching of the cement particles over time (lower) (Draganovic and Stille 2011)

2.1.8 Long slot

Long slot is another test method, developed by Draganovic and Stille (2014), to evaluate grout penetrability at conditions more similar to what occurs in a real fracture in rock compared to that in Short slot. The method comprised two parallel steel plates in the form of a slot (i.e. an artificial fracture) with more realistic geometries (Fig. 12-a). The slot was designed with 4 m length, 10 cm width, and a centrally collated 75-µm constriction. Similar to Short slot, the pressure source was a high-pressure gas tank providing an applied pressure of ≤ 20 bar. In this method, each experiment began by opening valve V4 that allowed the grout to flow through the slot. The intention was to monitor the filtration process at the constriction using the pressure gradient as an indication of filtration. Four pressure sensors were therefore located at the entrance of the slot, before and after the constriction, and immediately before the outlet, as can be seen in Fig. 12-a. Fig. 12-b shows the evolution of filtration and the pattern/streamlines proposed for the grout flow at the constriction over time. In Fig. 12-c, the pressure variation over time, anticipated at each pressure sensor, is presented for the grouting materials without filtration. Similarly, Fig. 12-d illustrates the expected pressure variation over time, but for the grouting materials with filtration. In this study, the constant pressure (over time) before and after the constriction was representative of non-filtration. However, the increase in pressure before the constriction and the decrease in pressure after it was an indication of filtration. In the meantime, any sudden reduction in pressure before the constriction was considered to be an indication of erosion.

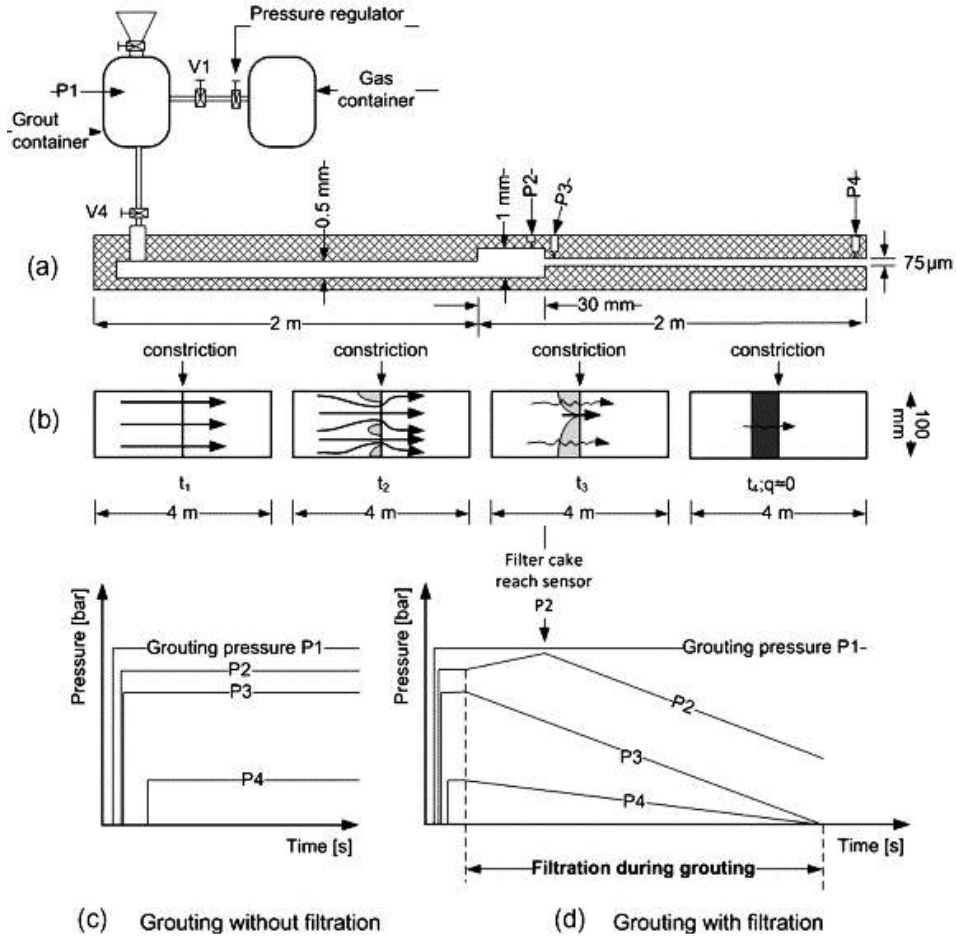

Fig. 12 Cross-section of Long slot (a), process of plug formation at the constriction (b) and pressure variation along the slot with and without filtration (c) and (d), respectively (Draganovic and Stille 2014)

2.2 Controversy in results – (the origins)

Based on the experiments conducted by Hjertström (2001) and Eriksson and Stille (2003), using the NES method and Penetrability meter, respectively, grout penetrability was reported independent of the water-to-cement (*w/c*) ratio. The results obtained from Filter pump, Sand column, Smooth slot, and Short slot, however, showed that the increase in *w/c* ratio improved grout penetrability (Hansson 1995; Eklund and Stille 2008; Axelsson et al. 2009; Draganovic and Stille 2011). In the experiments conducted by Hansson (1995) using the Smooth slot and Filter pump, use of super-plasticizer showed an increase in grout penetrability. In the experiments performed using Penetrability meter, on the other hand, Eriksson and Stille (2003) illustrated that use of super-plasticizer had no considerable effect on grout penetrability. These controversies and disagreements were probably due to the fact that the methods were designed based on different assumptions, limitations, and test conditions. They

might also be a result of deficiencies in their test set-ups, procedures, and/or evaluation methods. Some of the discrepancies and deficiencies can be summarized as follows:

2.2.1 Difference in the geometries and the filtration mechanisms

Sand column, Pressure chamber, and Filter press were more applicable to evaluate grout penetrability through a porous medium such as the soil and sand than a real fracture in rock. The corresponding reason, as discussed by Draganovic and Stille (2011), was the difference between the geometries and the filtration mechanisms through those media. The filtration mechanism assumed in the design of Filter press was the water loss through the fracture walls (See Fig. 3) being based on the porosity of the rock matrix and the presence of the micro-cracks (Gandais and Delmas 1987). This suggests that no filtration of the cement particles should appear in the fractures with impermeable walls, where there is no way for water to be lost through the walls. However, filtration was clearly observed in the results of the experiments conducted using Short slot, Long slot and PenetraCone with impermeable steel walls (Draganovic and Stille 2011, 2014; Axelsson and Gustafson 2010). This is contradictory to the preliminary assumption of Gandais and Delmas (1987) concerning the mechanism of the filtration in Filter press.

The mechanism of the filtration in the methods using the mesh geometry, e.g. in Filter pump and Penetrability meter, was best correlated to the clogging at the surface of a porous medium such as soil and sand. The filtration mechanism in the methods using the slot geometry, e.g. in the NES and Nobuto methods, and PenetraCone was more similar to the filtration at the entrance of a fracture. In Short slot and Long slot, however, the filtration occurred within a fracture due to the arching/bridging of the cement particles at the constrictions (Draganovic and Stille 2011, 2014). Furthermore, the probability of filtration in the mesh geometry was higher than that in the slot geometry. This was suggested by Eklund and Stille (2008), due to the support of the plug formation in the mesh geometry from four sides compared to that in the slot geometry, which was supported from only two sides. However, based on engineering judgement, the grout flow and the filtration process in the slot geometry was considered to be more realistic compared to what occurs in a real fracture in rock (Draganovic and Stille 2011, 2014).

2.2.2 Difference in the applied pressures

According to the literature, Sand column, Pressure chamber, and Filter press were designed to examine grout penetrability at pressures ≤ 2.6 bar, whereas the pressures commonly applied in Filter pump and Penetrability meter were approximately 0.5 and 1 bar, respectively. In comparison to these, the maximum pressure capacity in NES, PenetraCone, Short slot, and Long slot was ≤ 20 bar. However, this capacity in the Nobuto method was ≤ 50 bar.

As described by Eriksson et al. (1999), Hjertström (2001), Nobuto et al. (2008), Draganovic and Stille (2011), Stille et al. (2012) among others, the increase in pressure improves grout penetrability. This suggests a considerable difference between the results of the methods operating at a significantly wide range of the applied pressure (0.5-50 bar).

2.3 Comparison of Filter pump and Penetrability meter with Short slot

In order to distinguish the parameters governing grout penetrability measurement and determine the most reliable test methodology, three of the existing methods were selected for deeper comparison. Filter pump and Penetrability meter, as two of the most commonly used

methods in the Swedish grouting industry, were compared against Short slot with a geometry that was more realistic, using an evaluation method that was more accurate, and under test conditions that were much closer to the rock grouting conditions in the field.

In this comparison, the results of the experiments conducted using Filter pump and Penetrability meter were in disagreement with the results obtained from Short slot. The results were also associated with some uncertainties. These disagreements and uncertainties were, however, in conjunction with either of the parameters influencing grout penetrability or a combination of them, the most significant of which were identified as the applied pressure, the grout volume, the constriction geometry, and the evaluation method. These parameters should thus be considered with caution when evaluating the reliability and functionality of the instruments to obtain a more realistic measurement of grout penetrability.

2.3.1 Uncertainties and disagreements associated with the applied pressure

One of the first origins of the uncertainties, seen in the results of the experiments conducted using Filter pump, was probably the operator-dependency of the applied pressure. The pressures applied in different experiments using Filter pump were definitely not identical due to the manual performance of the experiments (i.e. pulling the handle of the instrument to suck the grout inside the tube by hand). This was more discernible when the experiments were performed by different operators or even an exhausted operator in consecutive tests.

According to Hansson (1995), the regular pressure applied in Filter pump was somewhat less than 0.5 bar. In Penetrability meter and Short slot, the pressure applied was, however, normally set to 1 and 15 bar, respectively (Eriksson and Stille 2003; Draganovic and Stille 2011). It is quite well known that the increase in pressure improves grout penetrability (Eriksson et al. 1999; Hjertström 2001; Nobuto et al. 2008; Draganovic and Stille 2011; Stille et al. 2012). This is due to the fact that the rise in pressure reorients the cement particles in the unstable arches and increases the potential for erosion of the unsettled filter cakes. This implies that measurement of grout penetrability is undeniably dependent on the grouting pressure and the experiments conducted on identical grout samples but at different pressures should definitely yield diverse or even contradictory results. Therefore, the considerable difference between the pressures applied in the methods selected in this study (0.5-15 bar) was clearly one of the origins of the disagreement in the results.

2.3.2 Disagreements associated with the grout volume

According to Hansson (1995), the maximum grout capacity in Filter pump was somewhat less than 0.3 l. In Penetrability meter, the capacity of the grout tank was approximately 5 l, whereas the maximum grout volume specified for each experiment was only 1 l (Eriksson and Stille 2003). In Short slot, the grout tank capacity used in each experiment was, however, 2.6 l (Draganovic and Stille 2011). As discussed by Eriksson and Stille (2003) and Eklund and Stille (2008), the grout filtration tendency is rationally increased by increasing the volume of the grout passed through a mesh filter. This is due to the fact that the higher the grout volume the higher the potential for accumulation and clogging of the cement particles and clusters at the constrictions. Therefore, the difference between the grout volumes used in the methods selected in the present study (0.3-2.6 l) was also an origin of the disagreement in the results, disregarding the effects of the uneven pressures and geometries.

2.3.3 Disagreements associated with the constriction geometry

In Penetrability meter and Filter pump, the length of the constrictions against the grout flow (i.e. the thickness of the woven metal mesh filter) was at most 100 μm, depending on the thickness of the wires used in the mesh filters (Hansson 1995; Eriksson and Stille 2003). In Short slot, the corresponding length (i.e. the length of the slot after reducing the aperture) was approximately 10 mm (Draganovic and Stille 2011). This was almost 100 times longer than that in Penetrability meter and Filter pump. The friction between the constriction walls and the grout, resisting against the grout flow along the mesh filter/constriction in both Penetrability meter and Filter pump, was therefore anticipated to be negligible compared to that in Short slot. Furthermore, the total effective area (i.e. the area of the opening minus the thickness of the wires produced the mesh filter) in both Penetrability meter and Filter pump was much larger than the area of the constriction in Short slot. In addition, as discussed by Eklund and Stille (2008), the potential for filtration in the methods using the mesh geometry was higher compared to that in the methods that used the slot geometry. These were possibly other reasons for further disagreements when examining identical grout samples using the selected methods.

2.3.4 Uncertainties associated with the evaluation method

Measurement of grout penetrability in terms of b_{min} and b_{crit}, developed by Eriksson and Stille (2003), has been one of the most commonly used criteria in the Swedish grouting industry over the past decade (Draganovic and Stille 2014). To determine these parameters, the volume of the grout passed through each filter plotted against the corresponding filter width has normally been employed in the experiments using Penetrability meter and Filter pump. The uncertainties involved become more discernible using mesh sizes sufficiently close to b_{crit} when following a stepwise bottom-up approach (i.e. when increasing the mesh sizes in consecutive tests). This can be visualized in the schematic depiction of the weight-time measurement presented in Fig. 13. When the mesh sizes are sufficiently close to b_{crit}, as shown in tests 5 and 6, despite the slight filtration (i.e. the minor deviations of the gradient shown as blue lines), the remaining opening is nonetheless large enough to let the entire specified grout volume pass through. Therefore, using the volume of the passed grout to determine grout penetrability, the evaluated b_{crit} might be smaller than the real value according to the definition (e.g. equal to the mesh size in test 5). However, using the weight-time measurement instead results in a larger b_{crit} with no filtration at all (e.g. equal to the mesh size in test 7). This should be considered with caution in evaluation of the reliability of the methods developed to measure grout penetrability.

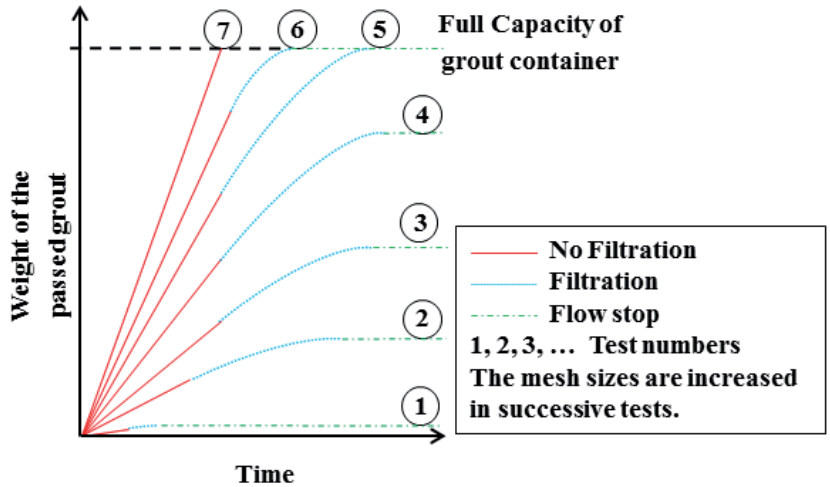

Fig. 13 Depiction of weight-time measurement to visualize the uncertainty in evaluation of b_{crit} using the total weight of passed grout

2.4 Adjustment of Filter pump and Penetrability meter

In part (a) of the study, the main objective was to provide a deeper understanding of the nature of grout penetrability and the corresponding governing factors. A second objective was to find the most reliable method for realistic measurement of grout penetrability. To have a reasonable comparison, Filter pump and Penetrability meter were both adjusted to operate using the evaluation methods and under test conditions as similar as possible to those in Short slot. The main remaining differences were: 1) the specified grout volume of 2.6 l in the modified Penetrability meter (MPM) versus 0.3 l in the modified Filter pump (MFP), 2) the mesh geometry used in MPM and MFP versus the slot geometry in Short slot (SS). The test apparatus, the experimental procedures, and the evaluation methods used in this part are summarized below.

2.4.1 Modified Filter pump (MFP)

The main objectives of adjusting Filter pump were: 1) to increase the applied pressure to 1 bar, 2) to exclude the operator-dependency of the pressure applied, 3) to employ the measure of weight over time as the evaluation method, and 4) to improve the repeatability of the method. A mass of 20 kg was therefore employed to provide the specified pressure of 1 bar constantly during all experiments using a partially automated system as shown in Fig. 14. To register the grout weight over time, the grout pot used was suspended from a load cell. More details of the test set-up can be found in Ghafar et al. (2017a). In each test, the smallest mesh filter (26 µm) was normally used for the first trial. By releasing the mass, the grout from the grout pot was sucked into the instrument and the weight of the passed grout through the mesh filter was registered over time to monitor the filtration. This procedure was repeated with the enlarged mesh filters in the consecutive tests until no filtration was observed in the results of the weight-time measurement. In this method, the maximum mesh size with negligible passed grout represented b_{min}, whereas the minimum mesh size with no filtration at all was an indication of b_{crit} (Fig. 15).

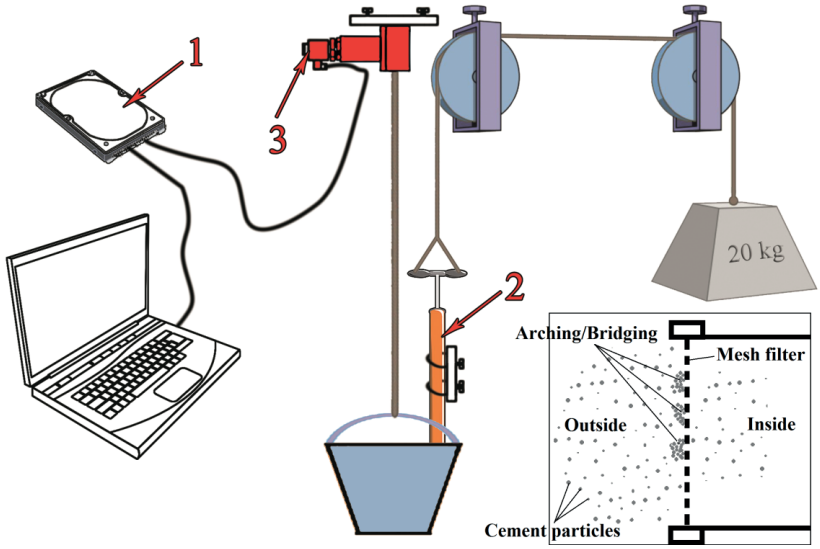

Fig. 14 Schematic view of MFP and details of arching/bridging at the mesh filter: 1) DAQ-data acquisition system, 2) filter pump, and 3) load cell

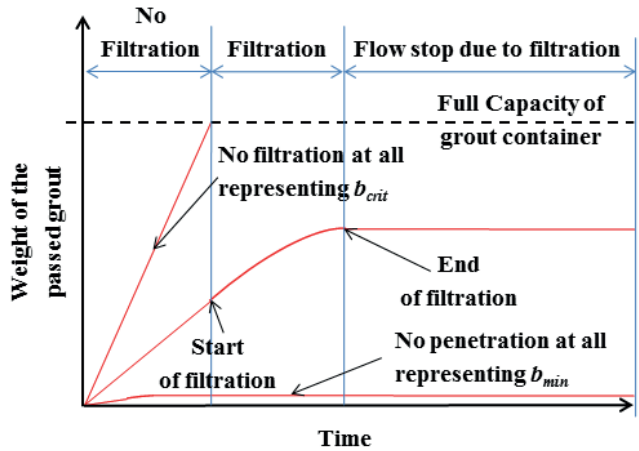

Fig. 15 Evaluation of b_{min} and b_{crit} using the weight-time measurement

2.4.2 Modified Penetrability meter (MPM)

The main objectives of adjusting Penetrability meter were: 1) to increase the specified grout volume in each experiment to 2.6 l, and 2) to employ the weight-time and the pressure-time measurements as the evaluation methods to monitor the filtration evolution. A grout tank (with 2.6 l capacity) was therefore suspended from a load cell to register the grout weight over time, as shown in Fig. 16. The grout tank was connected to a high-pressure gas tank (200 bar) through a regulator to provide a pressure of 1 bar constantly during all experiments. A pressure sensor was also added to the grout tank to record the pressure variation over time. Finally, a filter holder was attached to the bottom of the grout tank to replicate the filtration process as occurs in a regular Penetrability meter. In each experiment similar to MFP, the smallest mesh

size (26 µm) was regularly employed the first time. At the beginning, the grout in the tank was pressurized to 1 bar. By opening the outlet valve, the test was initiated, where the grout pressure and weight were recorded over time. This procedure was repeated with the enlarged mesh filters in the consecutive tests until no filtration was observed during the experiment. More details of the test apparatus and procedure can be found in Ghafar et al. (2017a). The methods employed to track the filtration process during the experiments using MPM were the weight-time and the pressure-time measurements described below:

- The weight-time measurement

The details of the weight-time measurement employed in MPM were exactly as described earlier in MFP.

- The pressure-time measurement

As seen in the schematic view of the pressure-time measurement in Fig. 17, by opening the outlet valve and beginning the grout flow a sharp drop in pressure occurs until the gas inflow compensates the grout discharge at the balance point. The pressure then remains constant, if the grout used is stable with no filtration-tendency similar to the results obtained from the water tests presented in detail in Ghafar et al. (2017a). In contrast, if the grout used is unstable with filtration-tendency, the size of the mesh openings and consequently the grout flow will be progressively reduced due to the filtration of the cement particles. A continuous pressure increase is therefore anticipated after the balance point. Using the pressure-time measurement, a mesh size providing a negligible pressure drop and an approximately immediate flow stop represents b_{min}, whereas a mesh filter that maintains the pressure at a constant level after the balance point represents b_{crit} (Fig. 17).

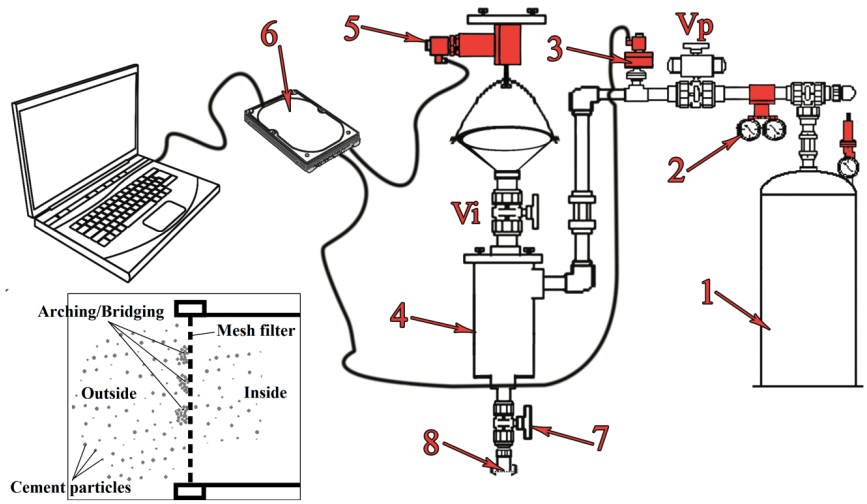

Fig. 16 Schematic view of MPM: 1) Gas tank, 2) pressure regulator, 3) pressure sensor, 4) grout tank, 5) load cell, 6) DAQ-data acquisition system, 7) outlet valve, 8) filter holder and mesh filter

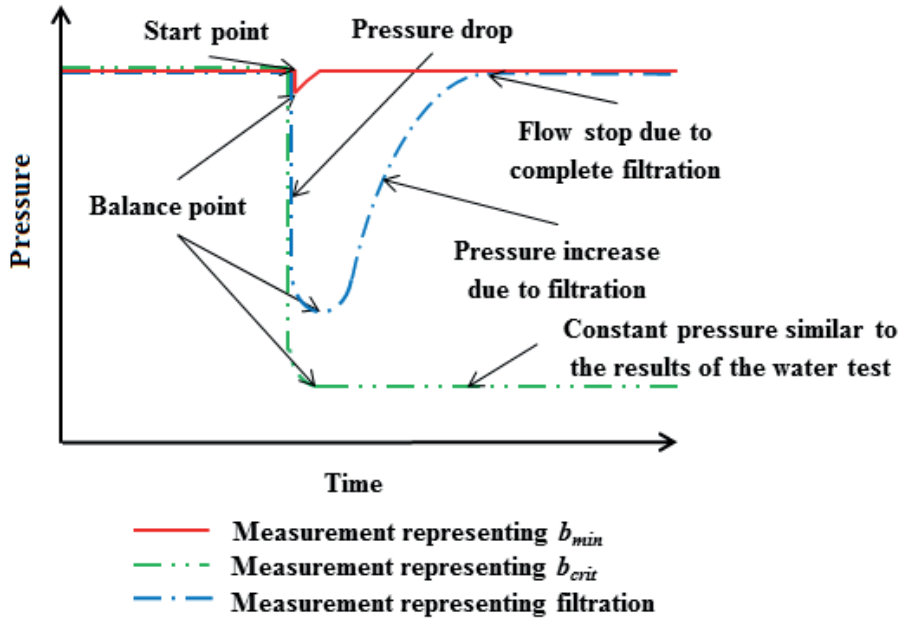

Fig. 17 Depiction of pressure-time measurement to monitor the filtration and evaluate b_{min} and b_{crit}

2.4.3 Short slot (SS)

The test apparatus, the procedure, and the evaluation method employed in the experiments using SS were exactly as presented earlier in this thesis. More details of the test set-up and procedure can be found in Draganovic and Stille (2011).

2.4.4 Materials, mixing process, and test plan

The grout used in part (a) of this study was prepared based on a commonly used recipe in the Swedish grouting industry. It contains INJ30 as cement from Cementa AB with d_{95} of 30 µm (i.e. at least 95% by weight of the cement particles pass through a 30 µm sieve), iFlow-1 as super-plasticizer from Sika AB with 0.5% concentration, using 0.8 water-to-cement ratio (w/c).

To mix the materials, a hand-mixer was used first to premix the scaled cement with water. A rotor-stator lab mixer was then employed to disperse the cement particles thoroughly within the suspension at 10,000 rpm for 4 minutes. The super-plasticizer was added to the suspension after 1 minute of mixing. The prepared grout was subsequently used to start each test immediately, according to the test plan presented in Table 1. More details concerning the materials, equipment, mixing process and test plan can be found in Ghafar et al. (2017a).

2.5 Summary of the results and discussion

The results of the penetrability measurement in terms of b_{min} and b_{crit} obtained for the examined grout using ordinary Filter pump (OFP), MFP, MPM, and SS with the differences and deficiencies described earlier are summarized in Table 2.

The results are further discussed in the following subsections with respect to the governing origins of the uncertainties and disagreements regarding grout penetrability measurement to provide a better understanding of the nature of grout penetrability and a reasonable evaluation of the reliability and functionality of the methods. More details and an interpretation of the results can be found in Ghafar et al. (2017a).

Table 1 Test plan

Test group	Pressure (bar)	Test device	Evaluation method	No. of repetitions with every mesh size											No. of repetitions with every slot size					
				26 µm	35 µm	43 µm	54 µm	61 µm	77 µm	90 µm	104 µm	122 µm	144 µm	200 µm	43 µm	50 µm	70 µm	84 µm	169 µm	177 µm
1	1	OFP	WT	1	4	4	4	3	3	2	-	-	-	-	-	-	-	-	-	-
2	1	MFP	WT	-	4	3	3	3	3	2	1	2	1	-	-	-	-	-	-	-
3	1	MPM	WT	-	2	2	2	-	3	1	2	1	3	-	-	-	-	-	-	-
4	1	MPM	PT	-	2	3	3	-	1	-	3	-	3	1	-	-	-	-	-	-
5	1	SS	WT	-	-	-	-	-	-	-	-	-	-	-	-	-	1	-	1	3
6	15	SS	WT	-	-	-	-	-	-	-	-	-	-	-	1	3	1	-	-	-
			Sum=	1	12	12	12	6	10	5	6	3	7	1	1	3	2	-	1	3
			Total No.= 85																	

OFP: Ordinary Filter Pump
MFP: Modified Filter Pump
MPM: Modified Penetrability Meter
SS: Short Slot
WT: Weight-time
PT: Pressure-time

Table 2 Summary of the results in terms of b_{min} and b_{crit}

Test device	Evaluation method	Pressure (bar)	b_{min} (μm)	b_{crit} (μm)
OFP	T	1	35	77
OFP	W	1	35	90
MFP	T	1	43	61
MFP	W	1	43	77
MPM	W	1	43	200
MPM	P	1	35	200
SS	W	1	70	200
SS	W	15	26	50

OFP: Ordinary filter pump
MFP: Modified Filter pump
MPM: Modified Penetrability meter
SS: Short slot

T: Total volume of passed grout
W: Weight-time
P: Pressure-time

2.5.1 Uncertainties induced by the applied pressure

In the experiments using OFP, different measurements of penetrability can be obtained for the same grout due to the operator-dependency of the pressure applied. This can be seen in the uneven and unequal mass flow rates obtained in the experiments with 43 - 77 μm mesh filters in Fig. 18, but using the results of the weight-time measurement instead of the total volume of passed grout. In the experiments using MFP, the obtained results show that the uncertainties can be significantly reduced merely by a slight modification of the method (Fig. 19).

In table 2, comparison of the measures of b_{min} and b_{crit} obtained from SS at 1 and 15 bar pressures, i.e. 70 versus 26, and 200 versus 50 μm, respectively, shows the extent of the influence of the pressure applied even using the same instrument with the same grout volume, geometry and evaluation method. This suggests the potential influence of the unequal pressures applied in various methods in the contradictions reported in the results of the grout penetrability measurement.

In rock grouting in the field, the grout-driving pressure that is mobilized at the grout front has its maximum close to the entrance of the fracture (i.e. close to the grouting borehole). This pressure gradually decreases when the grout penetrates through the fracture due to the friction and filtration. This suggests that the grout penetrability properties deteriorate through the reduction in pressure along a fracture. Therefore, to obtain a reasonable evaluation of grout penetrability in a real fracture in rock, it is essential to determine the penetrability of the selected grout at both the maximum pressure applied in the grouting borehole and a minimum pressure. The minimum pressure can be defined as the grout's remaining pressure when the grout front reaches the maximum penetration length required. This pressure should theoretically be close to zero at dry condition or close to the groundwater pressure at fully saturated condition. This suggests that use of SS only at high pressures such as 15 bar as proposed by Draganovic and Stille (2011) may not yield a satisfactory result applicable in the field.

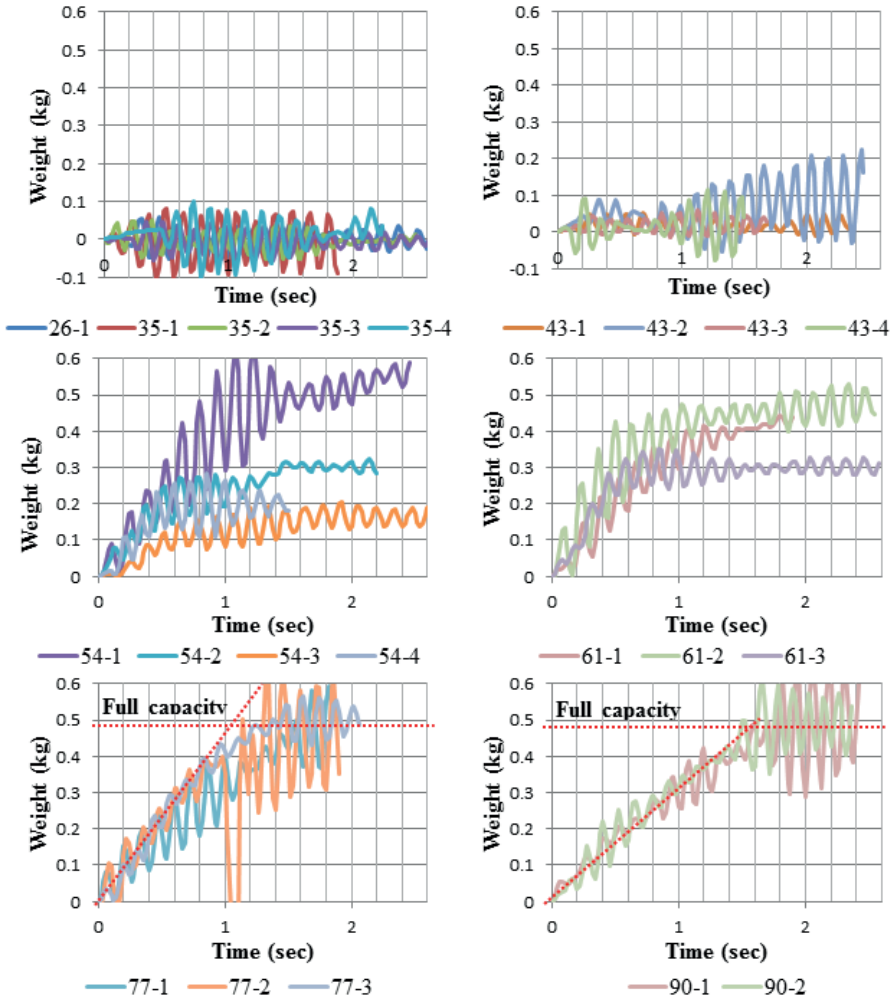

Fig. 18 Penetrability evaluated using OFP with 26-90 µm filters using the weight-time measurement

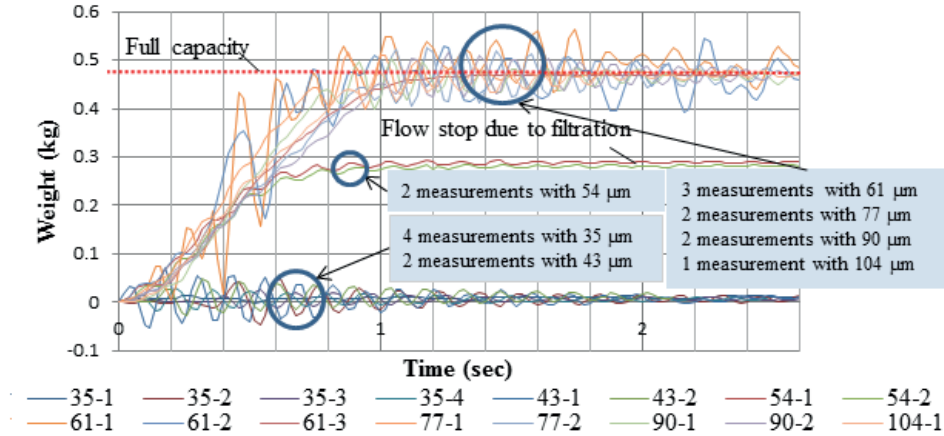

Fig. 19 Penetrability evaluated using MFP with 35-104 µm filters using the weight-time measurement

2.5.2 Uncertainties induced by the grout mass/volume

As can be seen from Fig. 20, the results of the weight-time measurement performed using MPM show that b_{crit} could be identified as 90 µm, if the grout mass used was somewhere between 1.0 and 1.5 kg. In the same figure, if the grout mass was ≤ 1.0 kg, b_{crit} could be even identified to be smaller, 77 µm. This is similar to the results obtained from MFP using the weight-time measurement with only 0.3 l (≈ 0.5 kg) grout capacity (Table 2). However, the results of the weight-time measurement conducted using MPM clearly show traces of filtration (i.e. the change in gradient) also in the experiments performed using 90-122 µm mesh sizes (Fig. 20). This is probably because the grout mass used in those experiments was ≥ 4.0 kg (2.6 l). Hence, b_{crit} of the examined grout using MPM is anticipated to be considerably larger (e.g. 200 µm). This implies that the difference between the specified grout mass/volume used in different methods can be another origin of the contradictions reported, which suggests the higher the grout mass/volume the larger the expected b_{crit}.

The grout volume required to obtain a sufficiently accurate measurement of grout penetrability can be determined in accordance with the grout volume required to fill a real fracture of average aperture size to the required distance. According to Grøv and Woldmo (2012), to obtain the required sealing in tunnels, achieving a penetration length of approximately 5-10 m is essential depending on the tunnel's application. Disk shape fractures with 50, 100, and 200 µm apertures and 5 m radius around a grouting borehole need a grout volume of approximately 10 l on average to be filled completely. However, this volume is needed for the two-dimensional flow condition. In order to estimate the grout volume required for measurement using SS with one-dimensional flow condition, the grout volume needed to fill only one-quarter of the disk shape fractures (with approximately one-dimensional flow condition) is sufficient. This is approximately 2.5 l, which is almost equal the maximum capacity of the grout tank in SS. In Filter pump and Penetrability meter, however, the designated grout volumes of approximately 0.3 and 1 l seem insufficient. This also contributes to underestimation of the measures of b_{min} and b_{crit} determined using Filter pump and Penetrability meter.

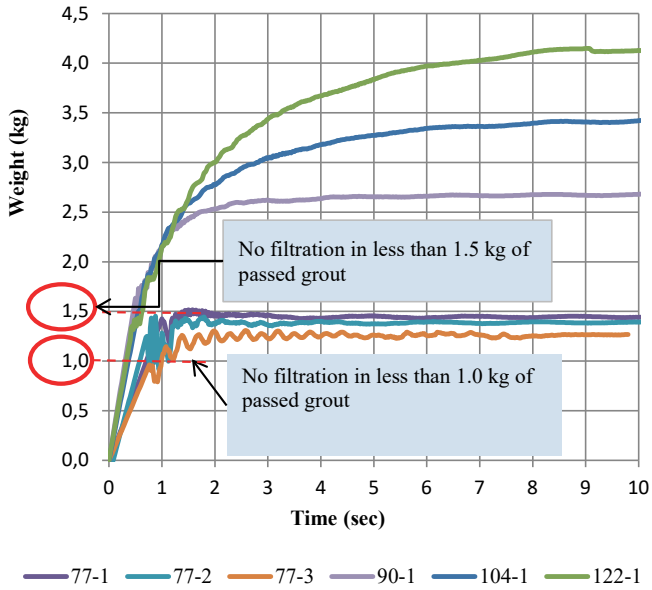

Fig. 20 Penetrability evaluated using MPM with 77-122 µm filters using the weight-time measurement

2.5.3 Uncertainties induced by the constriction geometry

As described earlier under MPM, the intention of the modification was to make its test conditions as close as possible to SS and use the same evaluation method. The grout volume and the applied pressure in both methods were thus 2.6 l and 1 bar, respectively. The main remaining difference between the two instruments was in the constriction geometry.

In MPM, the length of the constrictions against the grout flow (i.e. ≤ 100 µm) was approximately 100 times shorter than that in SS (i.e. ≈ 10 mm). The associated resisting friction against the grout flow and consequently the pressure loss along the constriction in MPM was therefore anticipated to be negligible compared to that in SS with the same size. This implies that a larger b_{min} is expected for the same grout in the experiments using SS compared to that using MPM. As shown in Table 2, the results verify that the evaluated b_{min} using SS (i.e. 70 µm) were larger than the results obtained from MPM (i.e. 35 and 43 µm) at 1 bar pressure. However, the estimated b_{crit} (i.e. 200 µm) that was similar in both methods shows that the diversity in the geometries is probably less significant in the large apertures that are sufficiently close to b_{crit} (Table 2).

2.5.4 Uncertainties induced by the evaluation methods

As seen previously in Fig. 18, the results of the experiments obtained from OFP with a 77-µm mesh filter using the weight-time measurement show some traces of filtration in the form of the change in the gradient of the mass flow rate. This suggests that a 77-µm mesh filter is not representative of b_{crit}. However, the results using a 90-µm mesh filter shown in the same figure, with negligible variation in the gradient, can be considered representative of b_{crit}. Using the total volume of passed grout instead, the filtration that occurred in the experiments with a 77-µm mesh filter could not be detected. Therefore, b_{crit} could be estimated to be 77 µm. This was due to the fact that the 77-µm mesh filter was sufficiently large to allow the whole capacity of the instrument to be filled with grout despite the existing filtration.

In a similar fashion, using the weight-time measurement in the experiments conducted using MFP with a 61-µm mesh filter, the results show some traces of filtration that could not be detected previously (Fig. 21). This clearly shows the extent of the influence of the sensitivity of the evaluation methods that should be carefully considered when choosing an appropriate instrument and method for more realistic evaluation of grout penetrability.

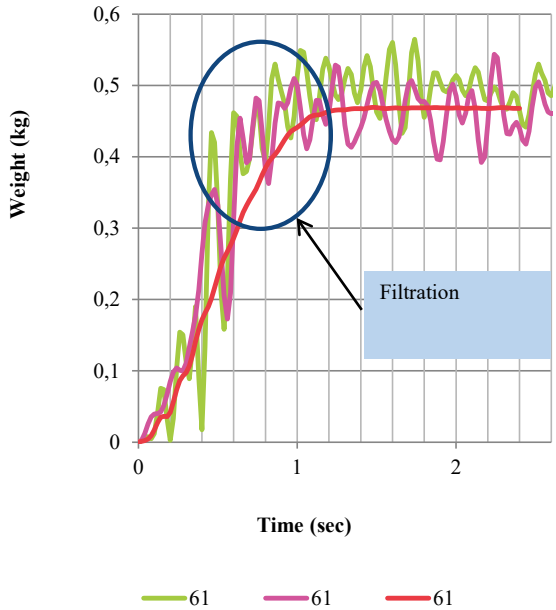

Fig. 21 Penetrability evaluated using MFP with 61-µm filter using the weight-time measurement

2.6 Conclusions

The main outcomes of part (a) can be summarized as follows:

- Diversity in the applied pressure, designated grout volume, and constriction geometry were found to be the governing origins of uncertainty and contradiction in the results of penetrability measurement instruments. Evaluation of b_{crit} at both low and high pressures (e.g. 1 and 15 bar) is essential. The higher the designated grout volume the greater the estimated b_{crit}. Finally, a rough estimation of the grout volume required for proper evaluation of grout penetrability is approximately 2.5 L.
- Application of Filter pump and Penetrability meter to measure grout penetrability in rock fractures is no longer recommended. Filter pump can, however, be used for quality control of cement and mixing process as suggested by Swedish standard SS-EN-14497.
- Short slot was found to be the best option among the three methods to measure grout penetrability in rock fractures due to more realistic geometry, a more accurate evaluation method, sufficient grout volume, and potential to operate at both low and high pressures.

3. Measurement of grout penetrability using Varying Aperture Long Slot (VALS) - Part (b)

Many scientists have spent much of their lives investigating the penetrability properties of cement-based grout in order to improve the grout spread into soil and the fractured hard rock effectively. The ultimate goal has always been to provide the sealing and the strength properties needed in underground infrastructures (Houlsby 1990; Lombardi 2003; Warner 2004; Gustafson and Stille 2005; Fransson 2008; Stille et al. 2012; Gustafson et al. 2013; Stille 2015; Ghafar et al. 2017a). Several methods have therefore been developed over the years to measure grout penetrability in both the lab and the filed. The diversity in their results indicates that these methods may not satisfactorily replicate the filtration process, particularly as occurs in the rock fractures, due to their specific design being based on unrealistic assumptions, limitations, and test conditions (Draganović and Stille 2011, 2014; Ghafar 2017a). In addition, a standardized method does not yet exist to evaluate grout penetrability into fractured hard rock. Part (b) of this study therefore aimed to contribute to a better test methodology for this purpose. A new experimental apparatus, the so-called varying aperture long slot (VALS), has therefore been developed based on assumptions, limitations and test conditions that are more realistic compared to those in the previous methods (Ghafar et al. 2017b). The method provided the possibility to study the influence of all parameters governing grout penetrability in fractured hard rock using an artificial fracture with 4 m length, 10 cm width, and varying constrictions (230-10 μm) to examine grout samples of any kind. This was made possible by monitoring the injected grout weight and the pressure before and after each constriction along the slot over time. The method operates at both static and dynamic pressures up to 15 bar. It has been designed based on the slot geometry with the filtration that occurs at the constrictions along the slot. The method is mainly used to determine grout penetrability in terms of b_{min} and b_{crit}.

3.1 A new method for more realistic measurement of grout penetrability

3.1.1 Test apparatus

A schematic view of the test set-up used is presented in Fig. 22. It comprised a high-pressure gas tank as the pressure source, a pressure regulator to maintain the required pressure (15 bar) at a constant level throughout the experiment, a 2.6-l capacity grout tank suspended from a load cell to register the grout weight, and a pressure sensor to monitor the grout tank pressure over time. The grout tank was then connected to VALS, which could be equipped with several pressure sensors before and after each constriction to monitor the filtration and erosion processes along the slot. More details of the test set-up can be found in Ghafar et al. (2017b).

3.1.2 Test procedure, materials, test plan, and evaluation methods

In this method, each test was normally begun by adjusting the pressure ($1 \leq P \leq 15$ bar). The materials used to prepare the grout samples were the same as in part (a) of the study, but using two recipes, R1 and R2, with w/c ratios of 0.8 and 2.0, respectively. The grout was then prepared based on a mixing process as described in part (a), according to the test plan presented in Table 3. Subsequently, the grout tank was filled with the prepared grout and pressurized. The test was then initiated by opening valve V12, while all other valves (V2–V11)

were closed except V1 that was kept open for air exhaust. The test apparatus was applicable in both dry and the fully saturated conditions. In each test, the injected grout weight, the pressure at the grout tank, as well as the pressures before and after the constrictions were registered over time to determine grout penetrability in terms of b_{min} and b_{crit} using only one batch of the grout mix. Using the online plot of the grout weight over time, one could figure out the right moments to switch the valves (e.g. closing V1 and opening V2, etc.). These moments were when the weight-time gradient tended to zero (i.e. when the grout flow through the slot stopped). By opening each valve, the grout flowed out if it was already there and eventually stopped due to the filtration; otherwise, one should proceed by opening the next valve. This process was continued (from V1 to V11) until no filtration (no variation in the weight-time gradient) was observed (Fig. 23). The apertures ahead of the valves with the first outflow and with no observable filtration represented b_{min} and b_{crit}, respectively. More details of the materials used, sample preparation, test plan and procedure, together with the other methods used to monitor the filtration and erosion at each constriction independently can be found in Ghafar et al. (2017b).

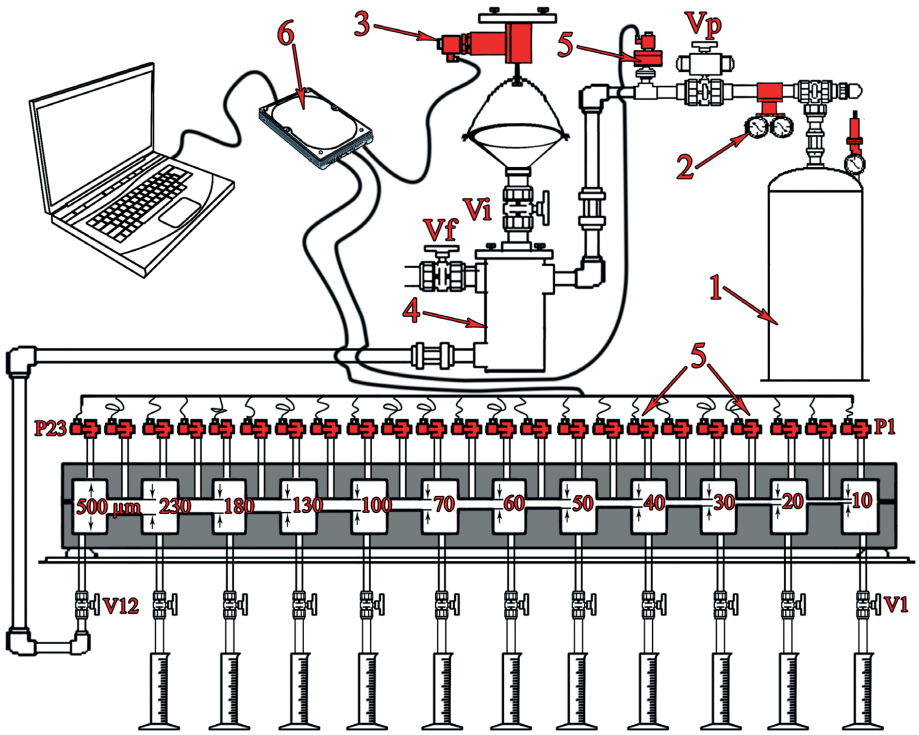

Fig. 22 Schematic view of VALS: 1) gas container, 2) pressure regulator, 3) load cell, 4) grout tank, 5) pressure transducers, 6) DAQ

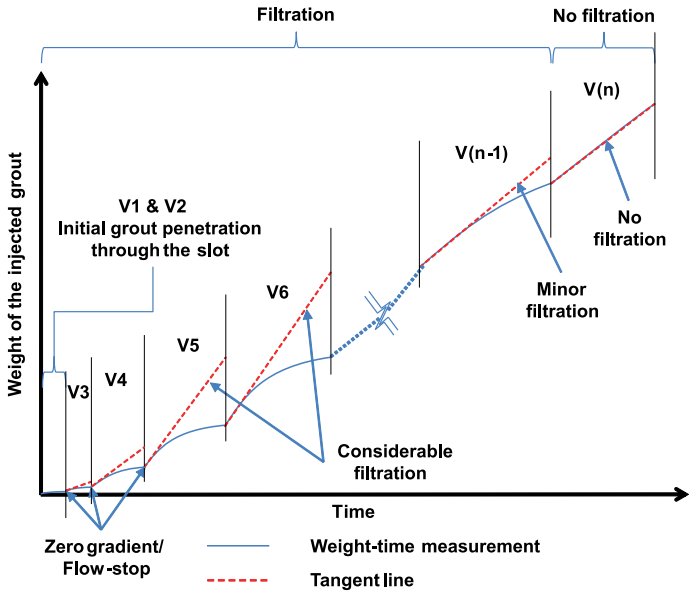

Fig. 23 Monitoring the filtration using the weight-time measurement

Table 3 Test plan

Test group	Recipe	No. of experiments	Pressure (bar)
G0	Water	10	15
G1	R1	2	1
G2	R1	3	15
G3	R2	2	1
G4	R2	3	15

3.2 Summary of the results and discussion

The results obtained from test group G0 (with water), test groups G1-G4 (with grout), and the associated calculations and interpretations are detailed in Ghafar et al. (2017b). As an illustration, the results of test G1-T1 conducted at 1 bar pressure and in dry condition using a grout mix based on recipe R1 are presented in Fig. 24. In this experiment, the first discharge occurred by opening valve V5 with 50-µm aperture. This suggests that the estimated b_{min} for the injected grout was approximately 50 µm. By opening the next valves (V6-V10), some traces of filtration (i.e. variation in the gradient of the weight-time measurement) were always observable. However, when valve V11 (with a 230-µm aperture) was opened, we could no longer identify any evidence of filtration. This implies that the estimated b_{crit} for the examined grout was approximately 230 µm (Fig. 24). To better distinguish the filtration that occurred when we opened valves V5-V10 consecutively, the same results are presented on a larger scale in Fig. 25. However, no evidence of filtration is observable when V11 (230 µm aperture) was opened.

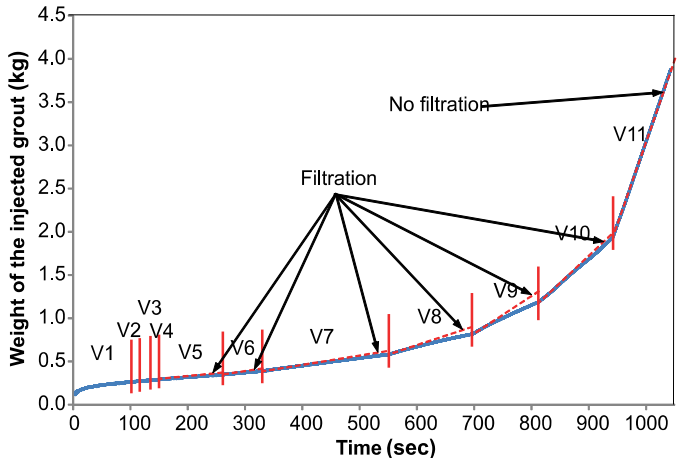

Fig. 24 Monitoring the filtration process in test G1-T1

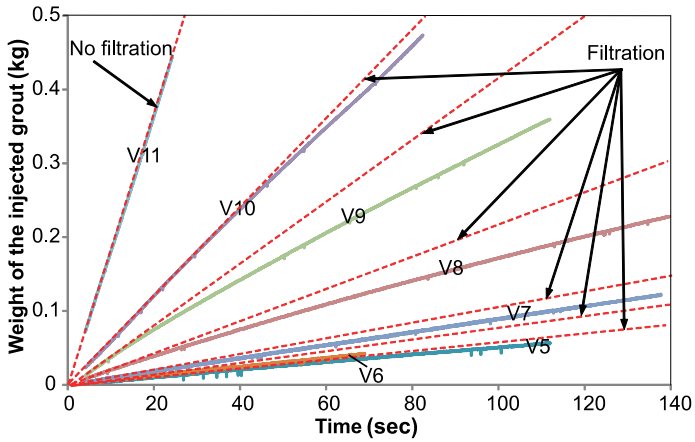

Fig. 25 Tracking the filtration in test G1-T1 by opening valves V5-V11

A summary of the results obtained from test groups G1-G4 (grout tests with 0.8 and 2.0 *w/c* ratios at 1 and 15 bar pressure) is presented in Table 4 to demonstrate the capability of the method to measure grout penetrability.

Comparison of the results of groups G1 and G3 performed on the grout samples using 0.8 and 2.0 *w/c* ratios at 1 bar pressure shows a reduction in b_{min} and b_{crit} from 50 to 40 μm and from 230 to 180 μm, respectively. This was expected due to the increase in *w/c* ratio. However, the corresponding effect on b_{crit} appeared to be stronger than b_{min} at this pressure. This might be because the estimated b_{min} (40 μm) was only slightly larger than *d95* of the cement used (30 μm). The increase in *w/c* ratio could therefore not affect the measurement of b_{min} significantly. Furthermore, the difference between the apertures of the first, second, and third constrictions (i.e. 230, 180, and 130 μm) is 50 μm in each case, whereas a smaller difference could provide more accurate measures for b_{crit} (somewhere between 230 and 180 μm).

Comparison of the results of groups G2 and G4 performed on the grout samples using 0.8 and 2.0 *w/c* ratios at 15-bar pressure shows a similar trend (a reduction from 40 to 30 μm) in the estimated b_{min}, while no reduction is observed in the estimated b_{crit}. This might be because the estimated b_{crit} (60 μm) is approximately twice the maximum particle size of the cement used. The corresponding improvement (i.e. the reduction in the estimated b_{crit}) might thus be so limited that it could not be distinguished by means of this method.

Comparison of the results of groups G1 and G2 performed on the same grout using 0.8 *w/c* ratio but at 1 and 15 bar pressures shows a considerable decrease in the estimated b_{crit} (from 230 to 60 μm) and a slight decrease in the estimated b_{min} (from 50 to 40 μm). The significant improvement in the estimated b_{crit} was expected due to the considerable increase in pressure. However, the minor influence on the estimated b_{min} was probably related to the maximum particle size of the cement used, as described earlier.

In addition, the pressure applied at the beginning of the slot in G1 (almost 1 bar) was anticipated to reduce through the slot down to approximately zero before the outlet. This means that the pressures at the locations where b_{crit} and b_{min} had to be evaluated were somewhat close to 1 and 0 bar, respectively. In similar fashion, the pressure applied at the beginning of the slot in G2 (almost 15 bar) was anticipated to reduce through the slot down to approximately zero before the outlet. Based on an analytical calculation similar to the one presented in Ghafar et al. (2017b), the pressures at the locations where b_{crit} and b_{min} had to be evaluated were calculated to be close to 13 and 7 bar, respectively. The pressure increase between test groups G1 and G2 at the locations where b_{crit} and b_{min} were evaluated therefore varied from almost 1 to 13 bar (≈12 bar) and from almost zero to 7 bar (≈7 bar), respectively. This reveals an approximately double increase in pressure (from G1 to G2) when estimating b_{crit} compared to b_{min}. This is also related to the significant reduction in b_{crit} from 230 to 60 μm (at a pressure increase of approximately 12 bar) in comparison to the slight reduction in b_{min} from 50 to 40 μm (at a pressure increase of only 7 bar).

Comparison of the results of groups G3 and G4 performed on the same grout using 2.0 *w/c* ratio but at 1 and 15-bar pressures again shows a considerable decrease in the estimated b_{crit} (from 180 to 60 μm) and a slight decrease in the estimated b_{min} (from 40 to 30 μm). This was for reasons similar to those described earlier in this section.

Table 4 Summary of the results obtained from test groups G1-G4

Group	Test No.	Grout recipe	w/c	Pressure (bar)	Grout penetrability (μm)	
					bmin	*bcrit*
G1	G1-T1 G1-T2	R1	0.8	1	50	230
G2	G2-T1 G2-T2 G2-T3	R1	0.8	15	40	60
G3	G3-T1 G3-T2	R2	2	1	40	180
G4	G4-T1 G4-T2 G4-T2	R2	2	15	30	60

3.3 Conclusions

The outcomes of part (b) can be summarized as follows:

- Varying aperture long slot (VALS) is a new lab-scale test apparatus developed to replicate the grouting operations in fractured hard rock based on assumptions, limitations, and test conditions that are considered to be more realistic compared to the existing methodologies.
- The method was tested and the results were in agreement with the acknowledged facts in common grouting practice, such as improvement of grout penetrability due to the increase in water-to-cement (w/c) ratio and pressure.
- The method has the potential to investigate the fundamental behavior of rock grouting with varying parameters such as grouting pressure, volume, water-to-solid ratio, etc. under both static and dynamic pressure conditions up to 20 bar.

4. Improvement of grout spread using dynamic grouting technique - Part (c)

Cement-based grout is the most common material used in rock grouting. The main issue in application of cement-based grout, however, is filtration of the cement particles that restricts spread of the grout in rock fractures. Several filtration mechanisms have been defined by experts in the area, of which the arching/bridging of the cement particles and clusters at a fracture constriction are the most relevant in rock grouting. Another factor that significantly controls the grout spread is the grout rheology, i.e. the viscosity and the yield stress. Several researchers have therefore aimed to improve the grout spread in rock fractures by influencing the grout-rheological and filtration properties. The grout properties might, however, be influenced by many parameters. The parameters that ultimately control the grout spread are the applied pressure, water-to-cement ratio (w/c), cement grain size and distribution curve, additives and admixtures, cement storage time, mixing time and waiting time after mixing, and finally mixer type, size, and speed.

In part (c) of this investigation, our focus was only to study the influence of the applied pressure on improving the grout spread. According to the literature, much work has been done concerning the application of the stepwise pressure increment. Use of the dynamic pressure (i.e. the high-frequency oscillating pressure) is another method that has been investigated with the aim of improving the grout spread in rock fractures since 1985. Besides the promising results obtained, the latter has, however, not yet been industrialized due to the limited efficiency and quick dissipation of the oscillation along a real fracture. In addition, the previous investigations conducted to study the influence of the dynamic pressure were all limited in the following issues (Ghafar et al. 2016):

- The pressure examined in almost all studies was a high-frequency oscillating pressure superimposed on an underlying constant pressure. Even though other alternatives to the dynamic pressure in terms of shape and frequency, e.g. the instantaneous and/or the ramp shape variable pressures, might show more efficiency, none has yet been examined (Fig. 26).
- The laboratory-scale tests were all conducted using parallel plates without constrictions and consequently with no influence of the filtration. The geometry used was, however, in contradiction with the geometry that might exist in a real fracture in rock with infinite irregularities.
- The mechanism of the improvement frequently described in all the investigations was only the reduction in grout viscosity due to the high-frequency oscillation. This was probably due to the fact that the resistance against the grout spread in the ideal parallel plates was highly dependent on the grout rheology. Other than the grout rheology, the grout filtration tendency was the other factor governing the grout spread. Therefore, to identify other alternatives to the mechanism of improvement, the filtration of the cement particles should also be replicated in the experiments using parallel plates with constrictions.
- The previous experiments were all conducted using apertures ≥ 100 μm, whereas successful grouting in the ≤ 70-μm fractures is necessary especially to provide the sealing required in areas such as nuclear/toxic waste repositories.

Accordingly, in order to increase the efficiency of the dynamic pressure on improving the grout spread, a solution might be to use a different shape and frequency of the applied pressure.

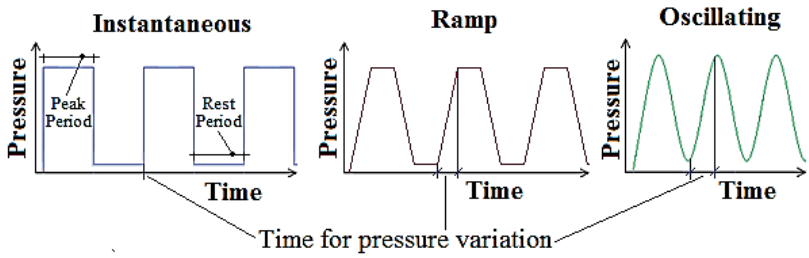

Fig. 26 Different alternatives to dynamic pressure

4.1 Application of rectangular pressure impulse

To improve the grout spread using dynamic grouting, the key factor is to control the filtration effectively. Accordingly, the acceleration, the magnitude of the pressure variation, and the durations at maximum and minimum pressures (i.e. the peak and rest periods) play essential roles (Fig. 26). These parameters depend on several features, the most significant being the shape of the applied pressure. In order to control the filtration, considerable erosion should be applied during the grouting process. This suggests using as high acceleration and magnitude of the pressure variation as possible. Furthermore, there are certain critical limits in selection of the peak and rest periods, above which a filter cake is expanded over the constriction to some extent that can no longer be eroded, and below which the durations are not adequate to obtain sufficient pressure variations (Fig. 27). This suggests using peak and rest periods as close as possible to the critical limits. In comparison between the oscillating, the ramp shape, and the instantaneous variable pressures (i.e. the rectangular pressure impulse), the last seems to be the best choice to maximize the efficiency of the dynamic grouting.

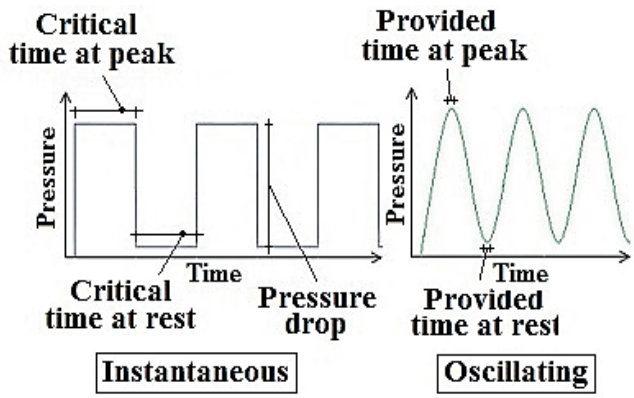

Fig. 27 Critical and provided times at peak and rest during the oscillating and instantaneous variable pressures

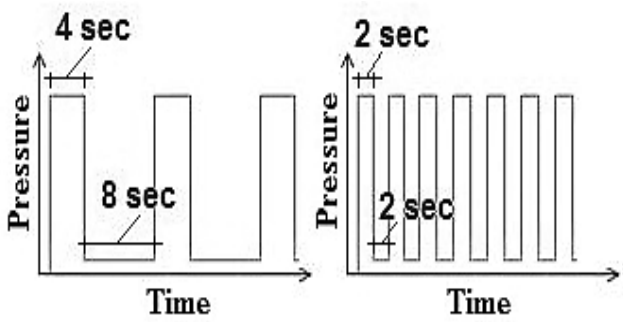

Fig. 28 Instantaneous variable pressure with peak/rest periods of 4 s/8 s and 2 s/2 s

4.1.1 Selection of the peak and rest periods

The critical peak and rest periods, which were highly dependent on the materials and the test set-up used, were identified in this study based on some preliminary tests under both static and dynamic pressure conditions. In these experiments, filtration was first observed after 4 sec. Approximately 8 sec were also required to obtain a relatively low pressure during the rest period. To prevent filtration before initiation and to obtain sufficiently low pressure during the rest period, our first choice for the peak and rest period was therefore 4 sec and 8 sec, respectively. To increase efficiency, better control the filtration during the peak period, and optimize the total duration, our second choice of peak/rest period was 2 s/2 s, respectively (Fig. 28). Reducing the peak/rest periods below that (2 s/2 s) was, however, found unproductive. The critical peak/rest periods for the materials and the test set-up used in this study were therefore identified as 2 s/2 s, respectively. More details concerning the selection of the peak/rest periods can be found in Ghafar et al. (2016).

4.1.2 Materials, mixing process, and test plan

The grout used in part (c) of this study was prepared based on the same materials, recipe, and mixing process described earlier in part (a). The experiments were then conducted under both static and dynamic pressure conditions using a maximum pressure of 15 bar, according to the test plan presented in Table 5. More details concerning the materials, mixing process and test plan can be found in Ghafar et al. (2016).

Table 5 Test plan

Test group	Number of tests	Slot size (μm)	Pressure type	Peak/rest period (sec)
C1	3	43	Static	-
C2	3	30	Static	-
V1	3	43	Dynamic	4 s/8 s
V2	3	30	Dynamic	4 s/8 s
V3	3	43	Dynamic	2 s/2 s
V4	2	30	Dynamic	2 s/2 s

4.1.3 Test apparatus, procedure, and evaluation methods

The test apparatus used in part (c) of the study consisted of a grout tank (2.6 l capacity) suspended from a load cell to register the grout weight over time. The pressure required was provided using a high-pressure gas tank (200 bar) and a regulator to maintain a static pressure of 15 bar during each experiment. A pressure sensor was also used to control the grout tank pressure. A pneumatic ball sector valve and a second pressure sensor controlled by a *PID*-control unit was then connected to the grout tank to convert the applied static pressure to an instantaneous variable pressure with specified durations of the peak/rest periods. A short slot was finally attached to the system to replicate the filtration at a fracture constriction (Fig. 29).

In each experiment, we first wrote a control script to specify the magnitudes and durations of the peak/rest periods. The grout in the tank was then pressurized to 15-bar pressure. To initiate the test, the script was run to open the valve instantaneously to start the grout flow.

After the predefined peak period, the valve was automatically closed. The result was a sharp drop in pressure followed by a gradual pressure decrease over the rest period. This process was repeated in consecutive cycles until the flow stopped (due to the filtration) or the completely discharge of the grout tank. More details of the test apparatus and procedure can be found in Ghafar et al. (2016).

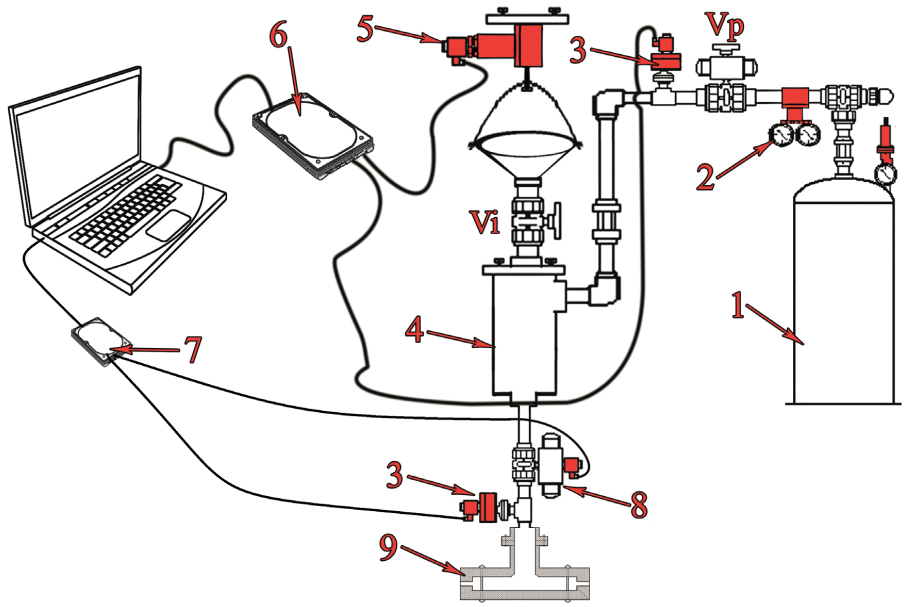

Fig. 29 Schematic view of the test set-up: 1) Gas tank, 2) pressure regulator, 3) pressure sensor, 4) grout tank, 5) load cell, 6) DAQ-data acquisition system, 7) PID control unit, 8) pneumatic ball sector valve, 9) Short slot

In this part, different methods were employed to illustrate and quantify the differences between the application of instantaneous variable pressure and static pressure to improve the grout spread. Those methods are briefly presented as follows. More detailed descriptions of the methods can be found in Ghafar et al. (2016).

- Total weight of passed grout

The method was used to determine the final differences between the static and the dynamic pressure results. However, using this method, it was not possible to observe the filtration and the erosion processes over time.

- Min-pressure envelope

The method was used to monitor the evolution of filtration and erosion throughout the experiment using the pressure-time diagram. The min-pressure envelope was a polyline obtained by connecting the vertices of the minimum pressures of the consecutive cycles (Fig. 30). Over this envelope, any upward and downward trends were representative of the filtration

and the erosion processes, respectively. The method was, however, unable to quantify the processes.

- Cycle mean flow rate (*CMFR*)

The method was used to quantify the filtration and erosion processes in each cycle to better distinguish between the effects of different peak and rest periods. The cycle mean flow rate (*CMFR*), defined as the mean value of the volumetric flow rate of the grout passed in each cycle, is determined using Eq. 1.

$$CMFR = \frac{V}{T} \qquad \text{Eq.1}$$

where V is the volume of grout passed per cycle and T the cycle duration.

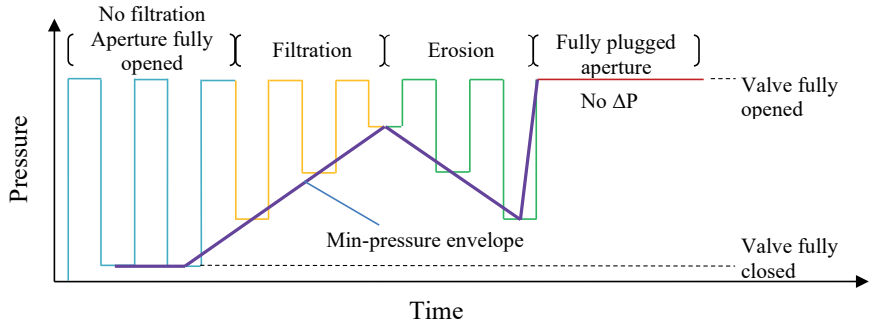

Fig. 30 Use of min-pressure envelope to visualize the filtration and erosion processes

4.1.4 Summary of the results and discussion

In part (c), we investigated the influences of instantaneous variable pressure with 4 s/8 s and 2 s/2 s peak/rest periods and the static pressure (15 bar) to improve the grout spread using a Short slot with 43 and 30 µm constrictions. The main objectives were to compare the effect of the pressures applied to improve the grout spread and to visualize and quantify the corresponding effects on the filtration and the erosion processes throughout the experiments. More details and an interpretation of the results can be found in Ghafar et al. (2016).

4.1.4.1 Comparison of the results obtained from 43-µm constriction

A summary of the results of the total weight of passed grout obtained from the experiments conducted using a 43-µm slot at both static and dynamic pressure conditions is presented in Table 6. As can be seen from the table, the average weights of the passed grout in groups V1 and V3 (using dynamic pressure with 4 s/8 s and 2 s/2 s peak/rest periods) were approximately twice the result obtained from group C1 (using static pressure). This shows the extent of the influence of the instantaneous variable pressure compared to that of the static pressure to improve the grout spread even through such a small aperture. However, the method (i.e. the total weight of passed grout) used for this evaluation was not able to distinguish the difference between the results of the peak/rest periods used. The method was also unable to visualize and quantify the filtration and erosion processes during each experiment.

Table 6 Results of the total weight of passed grout under both static and dynamic pressure conditions using a 43-µm slot

Test group	Test No.	Peak/Rest period (sec)	Weight of passed grout (kg)	Final tank condition	Average weight of passed grout (kg)	Improvement compared to the static pressure condition
C1 (static)	1	-	1.339	Not empty	1.932	-
	2	-	2.055	Not empty		
	3	-	2.402	Not empty		
V1 (dynamic)	1	4 s/8 s	4.189	Empty	4.271	2.2
	2	4 s/8 s	4.302	Empty		
	3	4 s/8 s	4.321	Empty		
V3 (dynamic)	1	2 s/2 s	4.093	Empty	4.072	2.1
	2	2 s/2 s	4.177	Empty		
	3	2 s/2 s	3.947	Empty		

Instead, using the min-pressure envelopes shown in Fig. 31, we visualized the filtration and erosion processes in consecutive cycles, respectively. In the top figure, the results of three experiments conducted using a 4 s/8 s peak/rest period showed random filtration and erosion processes (upward and downward trends) in different cycles of various intensities (gradient). This was an indication that the peak and rest periods were probably too long, allowing the filter cakes to occasionally expand over the constriction. The results of experiments conducted using 2 s/2 s peak/rest period (bottom figure), however, showed a gradual upward trend. This was an indication of the minor accumulation of the filtration in consecutive cycles due to better control of the filtration process. Nonetheless, the method used was not suitable for quantifying the improvements.

Finally, using the average *CMFR* shown in Fig. 32, we quantified and compared the resulting influences of the filtration and erosion that occurred in different experiments. In this figure, the average *CMFR* obtained from the experiments conducted using 2 s/2 s peak/rest periods ($(1.65 + 2.03 + 1.59)/3 = 1.76\ l/min$) was approximately 140% higher than that obtained from the tests performed using 4 s/8 s ($(0.57 + 0.81 + 0.78)/3 = 0.72\ l/\text{min}$). This means that the discharge of the grout tank was almost 140% faster in the experiments using 2 s/2 s peak/rest periods due to less accumulation of filter cakes and consequently a wider opening. This suggests that in the experiments using 2 s/2 s peak/rest periods the filtration was controlled better than in the experiments using 4 s/8 s.

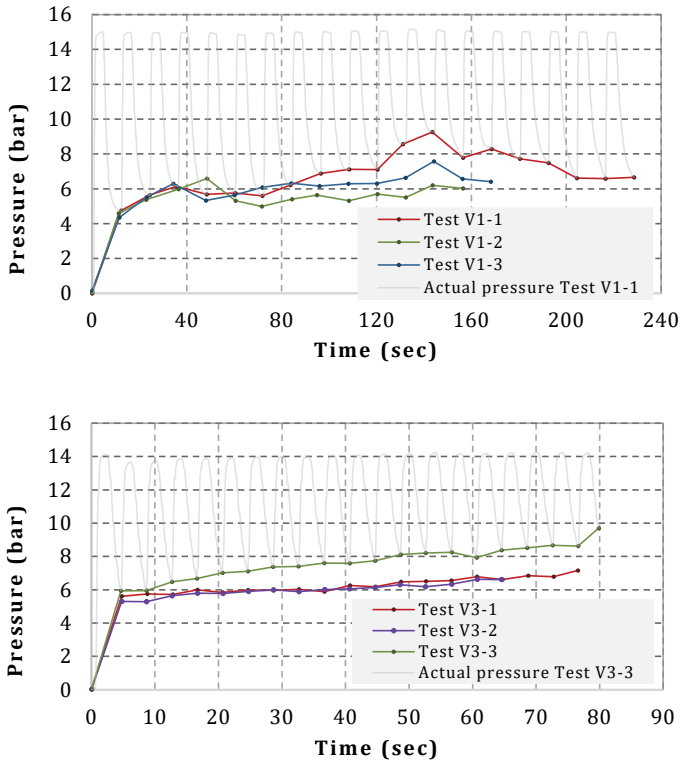

Fig. 31 Min-pressure envelopes obtained using 43-µm slot with 4 s/8 s (top) and 2 s/2 s (bottom) peak/rest periods

In the analysis described earlier, the entire cycle period was considered as the time for the pressure to act, but with different mean flow rates during the peak and rest periods. However, if one considers the duration of the peak period as the only time for the pressure to act (and disregarding the rest periods), the mean values of the sum of the peak periods in the experiments with 4 s/8 s and 2 s/2 s peak/rest periods are calculated to be 66.7 and 38 sec, respectively (Fig. 32). This suggests a 76% longer period for the pressure to act (for the experiments using 4 s/8 s) and consequently a larger volume of passed grout (if one assumes the same opening in both cases). However, the equal grout volumes (2.6 l) passed through the slot in both cases yield an average flow rate 76% higher for the experiments using 2 s/2 s peak/rest periods. This once again is related to less accumulation of filter cakes due to better-controlled filtration in the experiments using 2 s/2 s peak/rest periods.

As can be seen from the same figure, the considerably high *CMFR* obtained in the first cycle of each test (compared to that in the following cycles) was probably due to the severe filtration that occurred during the first cycle of each experiment. This suggests the significance of the first cycle in the application of instantaneous variable pressure to improve the grout spread effectively. In addition, the higher *CMFRs* in the first cycles of the experiments with 2 s/2 s peak/rest periods compared to that in the experiments with 4 s/8 s was an indication of lower filtration over the first cycles in the former case.

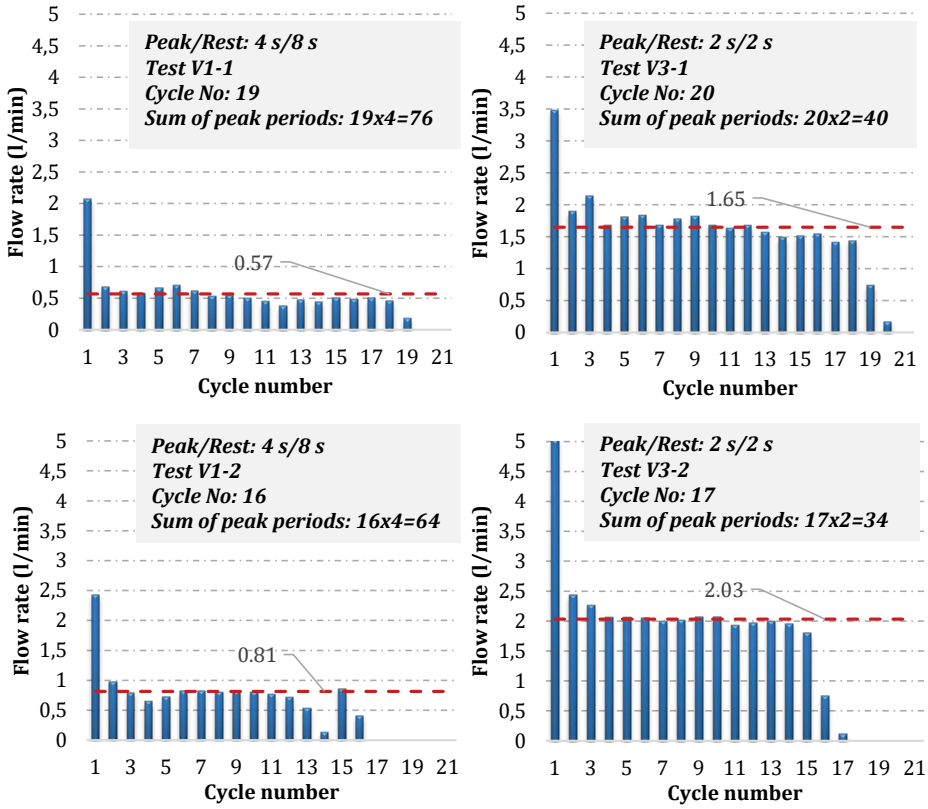

Fig. 32 Cycle mean flow rates (*CMFRs*) and average *CMFRs* for the experiments using 43-µm slot with 4 s/8 s and 2 s/2 s peak/rest periods

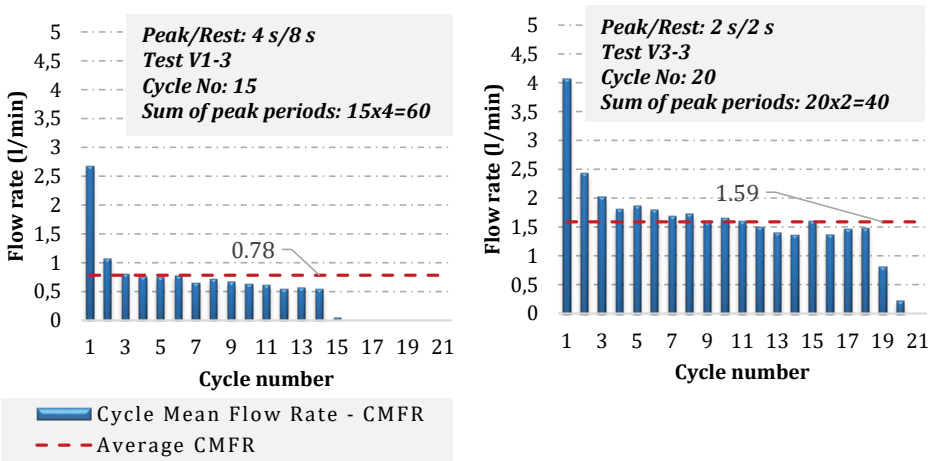

4.1.4.2 Comparison of the results obtained from 30-µm constriction

A summary of the results of the total weight of passed grout obtained from the experiments conducted using a 30-µm slot under both static and dynamic pressure conditions is presented in Table 7. In the table, the average weights of the passed grout in groups V2 and V4 (using 4 s/8 s and 2 s/2 s peak/rest periods) are approximately 3 and 11 times the result obtained from group C2. This shows the considerable influence of the instantaneous variable pressure especially using 2 s/2 s peak/rest periods compared to that of the static pressure to improve the grout spread even through a 30-µm aperture.

However, the min-pressure envelopes obtained from the experiments with 4 s/8 s peak/rest periods (See Fig. 33, top) showed severe filtration throughout the experiments with almost no sign of dominant erosion (downward trend). This once again was a clear indication that the selected peak and rest periods were extremely long. The result was accumulation of the filtration over the constriction until the flow stopped in a couple of cycles.

In contrast, the min-pressure envelopes obtained from the experiments with 2 s/2 s peak/rest periods (See Fig. 33, bottom) showed several cycles with erosion (downward trend). These cycles were the main reason for keeping a partially plugged constriction even with a 30-µm aperture open for a longer period to achieve more penetration.

Table 7 Results of the total weight of passed grout under both static and dynamic pressure conditions using a 30-µm slot

Test group	Test No.	Peak/Rest period (sec)	Weight of passed grout (kg)	Final tank condition	Average weight of passed grout (kg)	Improvement compared to the static pressure condition
C2(static)	1	-	0.441	Not empty	0.299	-
	2	-	0.181	Not empty		
	3	-	0.275	Not empty		
V2(dynamic)	1	4 s/8 s	0.852	Not empty	0.786	2.6
	2	4 s/8 s	0.824	Not empty		
	3	4 s/8 s	0.684	Not empty		
V4(dynamic)	1	2 s/2 s	2.679	Not empty	3.190	10.7
	2	2 s/2 s	3.702	Not empty		

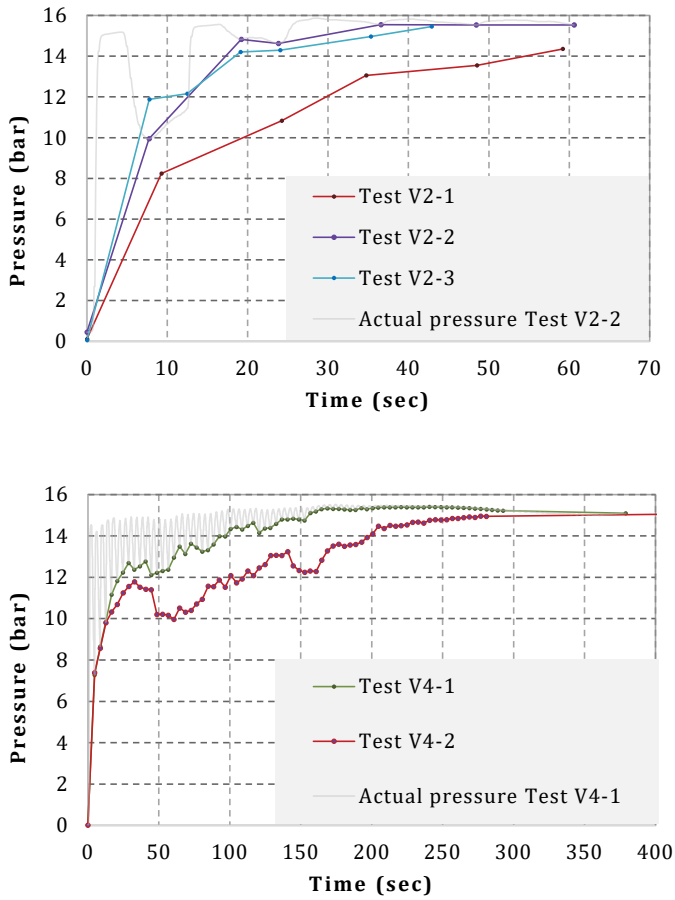

Fig. 33 Min-pressure envelopes obtained using a 30-µm slot with 4 s/8 s (top) and 2 s/2 s (bottom) peak/rest periods

In addition, the considerable difference between *CMFRs* in the first and second cycles in each test was again an indication of significant filtration within the first cycles (Fig. 34). Furthermore, the higher *CMFRs* in the first cycles of the experiments with 2 s/2 s peak/rest periods compared to that in the experiments with 4 s/8 s was an indication of lower filtration over the first cycles in the former case. This once again shows that the 2 s/2 s peak/rest period was closer to the critical values, resulting in better control on filtration and improved grout spread.

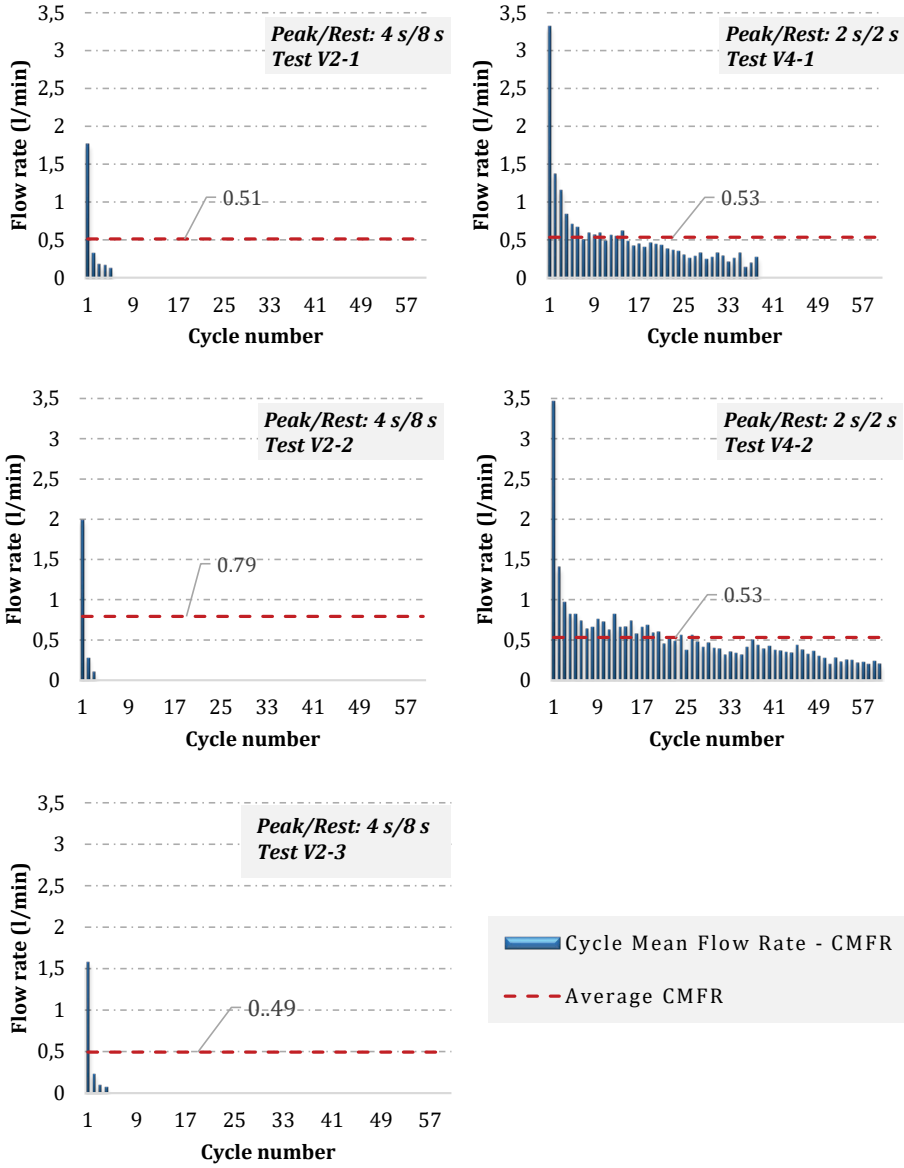

Fig. 34 Cycle mean flow rates (*CMFRs*) and average *CMFRs* for the experiments using a 30-µm slot with 4 s/8 s and 2 s/2 s peak/rest periods

4.1.4.3 Conceptual model of the mechanism of action

To interpret the mechanism of improvement of the grout spread using the instantaneous variable pressure, the flow types within the slot at various pressures during the peak and rest periods were calculated. The calculation was based on the flow equations between parallel plates for the selected material and test set-up (White, 1998). The results revealed a pressure of approximately 9 bar, above which the flow was turbulent and below which laminar. On this basis, depending on the extent of the pressure change over each cycle, two mechanisms of action were identified (Fig. 35):

- Major pressure variation (change between 15 and <9 bar)

As shown in Fig. 35a, since the pressure applied during the peak period is higher than 9 bar, the resulting flow velocity is high. Therefore, the Reynolds number calculated for the grout flow during the peak period represents the turbulent flow condition. This high pressure, however, significantly drops to less than 9 bar during the rest period. As a result, the flow velocity and consequently the associated Reynolds number both decrease. This suggests change of the flow type from turbulent to laminar during the rest period. The same process is repeated in consecutive cycles, where the variation in flow type between turbulent and laminar considerably changes the flow pattern. The cyclic change in the flow pattern is anticipated to increase the potential of erosion of any unstable filter cakes and improve the grout spread significantly.

- Minor pressure variation (change between 15 and >9 bar)

As shown in Fig. 35b, since the pressure applied during both the peak and the rest periods is higher than 9 bar, the flow type always remains turbulent with only a minor variation in the flow pattern (Fig. 35b). This suggests only a slight erosion of the produced filter cakes in consecutive cycles. Therefore, a limited efficiency is anticipated for the method with minor pressure variation.

The two proposed mechanisms of action can also be distinguished in our obtained results as described in detail in Ghafar et al. (2016).

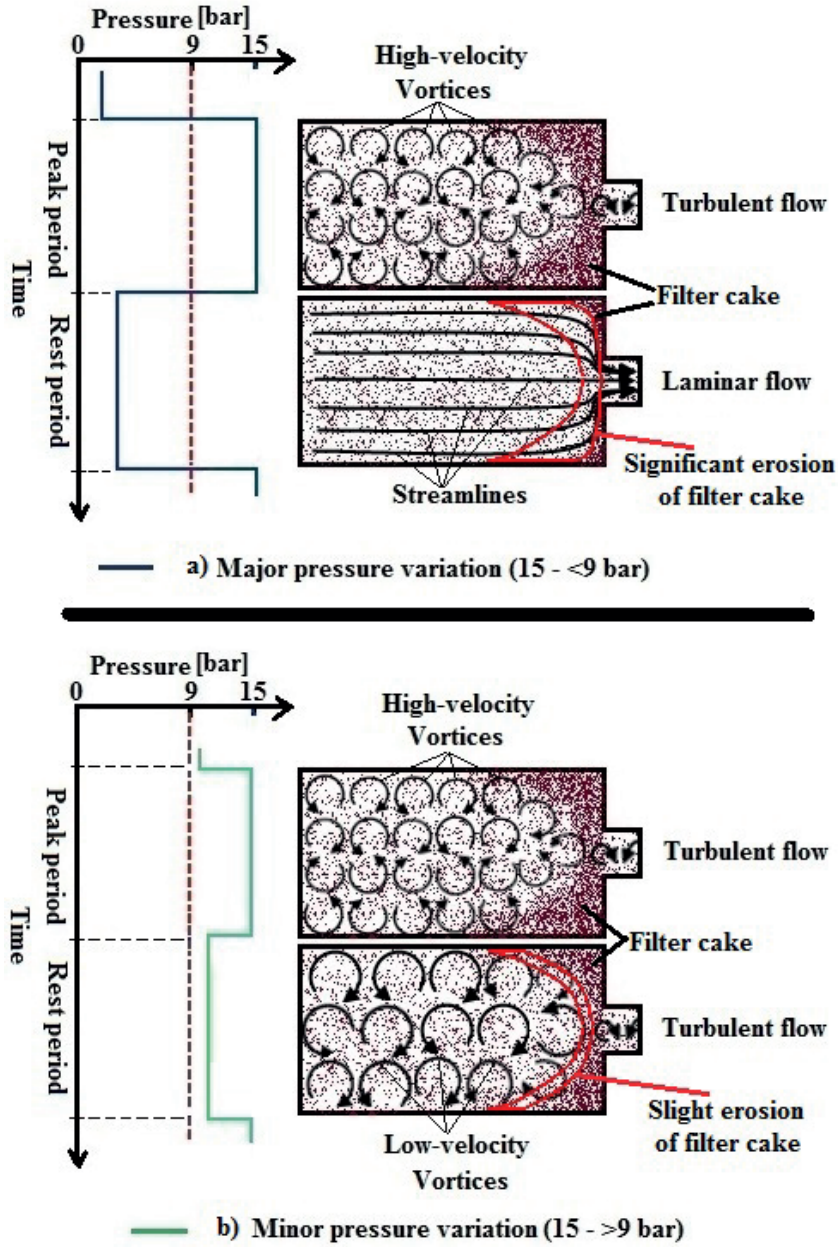

Fig. 35 Conceptual model of the mechanism of action

4.2 Dissipation of the pressure impulses along a fracture

In section 4.1, a low-frequency instantaneous variable pressure (i.e. a rectangular pressure impulse) was introduced to improve the grout spread. The aim was to achieve better control of filtration by gradual erosion of the filter cakes produced at a fracture constriction in consecutive cycles. The mechanism of action was interpreted as variation in the flow pattern due to the change in pressure and consequently the flow velocity. Two peak/rest periods (i.e. 4 s/8 s and 2 s/2 s) were examined using Short slot with 30 and 43 μm constrictions. The results showed significant improvement (up to 11 times), in particular in the experiments using 2 s/2 s peak/rest periods. However, dissipation of the pressure impulses along a fracture was nonetheless questionable. To investigate this in a considerably longer artificial fracture, the so-called VALS, the subject of part (b) of the study, was employed using 2 s/2 s peak/rest periods at a maximum pressure of 15 bar (Ghafar et al. 2017c). The main objective was to investigate how large the remaining amplitudes of the pressure impulses are at 2.0 and 2.7 m from the beginning of the slot with aperture ranges of 230-70 and 230-50 μm, respectively.

4.2.1 Materials, mixing process, and test plan

In this part of the study, the experiments were conducted using tap water (20°C) and a grout commonly used in the Swedish grouting industry prepared based on the same materials, recipe, and mixing process described earlier in part (a). The corresponding details as well as the measured rheological and bleeding properties of the prepared grout can be found in Ghafar et al. (2017c).

4.2.2 Test apparatus, procedure, and evaluation methods

The test apparatus used in this part of the investigation was similar to that in part (b) using VALS to mimic the grouting process in a longer fracture compared to that in Short slot. A three-way ball valve was located at the slot's entrance to convert the applied static pressure (15 bar) to an instantaneous variable pressure with 2 s/2 s peak/rest periods (Fig. 36). The VALS itself was equipped with pressure sensors, P1–P3, to register the pressure variation at 2.7, 2.0, and 0.0 m from the beginning of the slot, respectively, to study the dissipation of the pressure impulses and any filtration and erosion processes along the slot.

In each experiment, the grout/water in the tank was first pressurized to 15 bar. The test was initiated by frequently switching the three-way valve to either allow the grout to flow through VALS (outflow from valve V1) or lower the VALS's internal pressure to the atmospheric pressure (Fig. 36).

In order to visualize the dissipation of the pressure impulses along VALS, the magnitudes of the pressure variations registered by P1–P3 were compared. In addition, to monitor the evolution of filtration and erosion in consecutive cycles, the max-pressure envelope (i.e. a polyline obtained by connecting the vertices of the maximum pressures of the consecutive cycles) was employed. Over this envelope, any upward and downward trends were representative of the filtration and the erosion processes, respectively.

It should, however, be mentioned that a considerable volume of the grout used during the experiment flowed out when switching the three-way valve to reduce the slot's internal pressure to the atmospheric pressure. The injected grout volume through the slot was therefore not sufficient to study the influence of the applied pressure on the total volume of grout take.

However, the dissipation of the pressure impulses along VALS and the evolution of the filtration and erosion processes were studied. More details of the test apparatus, procedure, and evaluation methods can be found in Ghafar et al. (2017c).

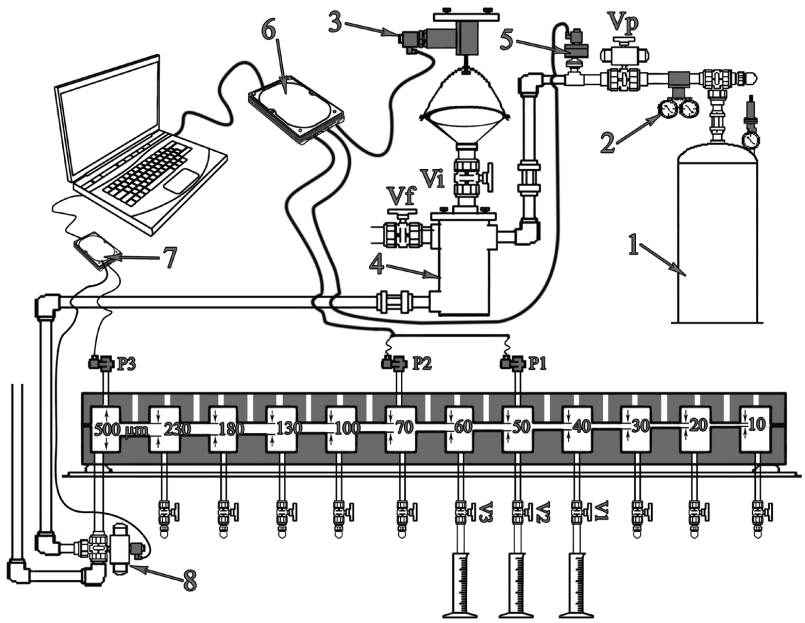

Fig. 36 Schematic view of the test set-up: 1) gas tank, 2) pressure regulator, 3) load cell, 4) grout tank, 5) pressure sensor, 6) DAQ, 7) PID-control unit, 8) three-way ball valve

4.2.3 Summary of the results and discussion

4.2.3.1 Analysis of the pressure impulse dissipation

Fig. 37 shows the results of the pressure-time measurement obtained from the water test. The initial pressure applied at the beginning of the slot, with a peak-to-peak amplitude of 14 bar, showed a dissipation of approximately 38% (registered by P2) over the first 2.0 m length of the slot with varying apertures of 230-60 µm at stabilized condition after 25 s. The initial applied pressure showed a dissipation of approximately 70% (registered by P1) along a 2.7 m length of the slot, with varying apertures of 230-40 µm. This indicates that the remaining amplitude of the pressure impulses after 2.0 and 2.7 m can be as large as 60% and 30% of the initial/applied amplitudes in the water test performed, respectively.

Fig. 38 shows the results of the pressure-time measurement obtained from the grout test. The initial pressure applied at the beginning of the slot showed a dissipation of approximately 54% (registered by P2) over the first 2.0 m of the slot with varying apertures of 230-60 µm at stabilized condition after 2 min. The initial applied pressure then showed a dissipation of approximately 75% (registered by P1) along a 2.7 m length of the slot, with varying apertures of 230-40 µm at stabilized condition after 3 min. The analysis shows that the remaining amplitude of the pressure impulses after 2.0 and 2.7 m can be as large as 46% and 25% of the initial/applied amplitudes in the grout test performed, respectively.

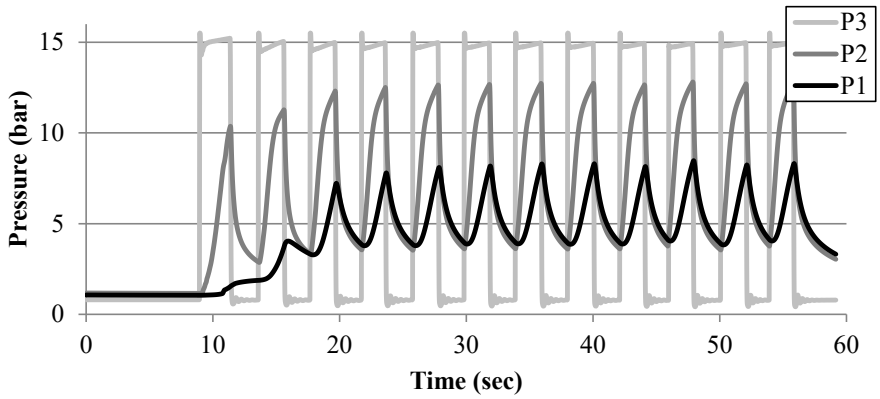

Fig. 37 Results of the pressure-time measurements using P1-P3 in water test with 2 s/2 s peak/rest periods (P1 and P2 are located before 40 and 60 µm constrictions, respectively)

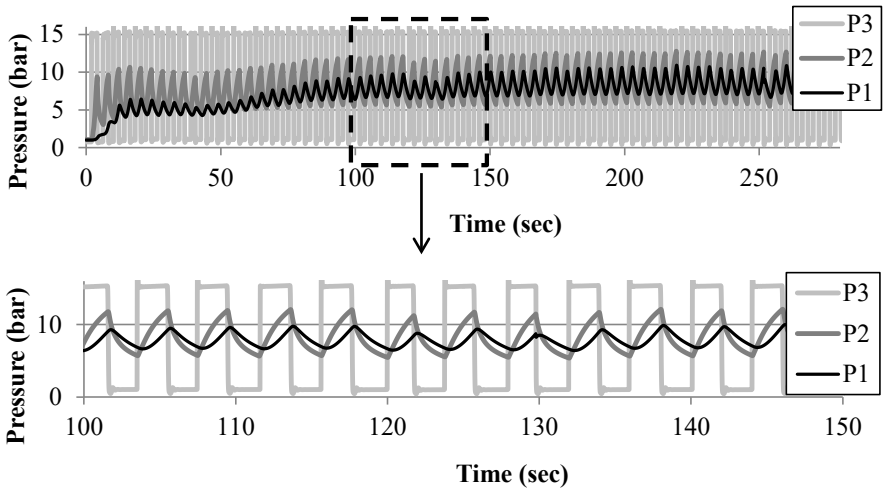

Fig. 38 Results of the pressure-time measurements using pressure sensors P1–P3 in grout test with 2 s/2 s peak/rest periods

4.2.3.2 Analysis of the max-pressure envelope

Fig. 39 shows the max-pressure envelopes obtained from the pressure-time measurements conducted at 2.0 and 2.7 m from the beginning of the slot during the water test. As can be seen, there is no trace of filtration/erosion (stabilized envelopes) after 25 s of injection as anticipated for water.

Fig. 40, however, shows the max-pressure envelopes obtained from the pressure-time measurements at 2.0 and 2.7 m from the beginning of the slot during the grout test. Five different periods can be distinguished in the envelopes: 0-20 s, 20-40 s, 40-120 s, 120-140 s, and 140-290 s. After initial filling of the slot during the first period (0-20s), both pressures P1 and P2 fell during the second period (20-40 s) due to the filtration at constrictions ≥ 70-µm. In the third period (40-120 s) both pressures increased in a similar way (almost linearly), most likely due to the filtration at the 40-µm constriction. In the fourth period (120-140s), both pressures fluctuated but with similar trends. This might also be an indication that several filtrations/erosions occurred at the 40-µm constriction. In the last period (140-290 s) the pressures were relatively stable with some minor fluctuations due to the eventual filtrations/erosions that kept the 40-µm constriction partially open for more penetration.

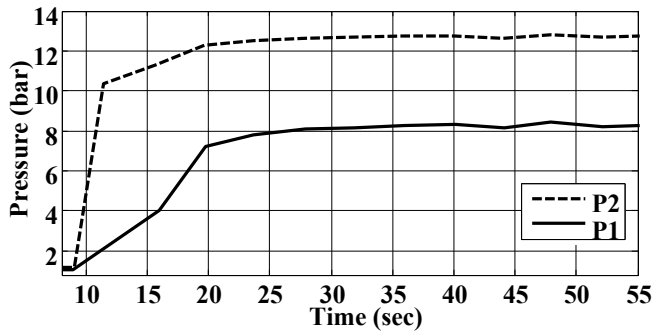

Fig. 39 The max-pressure envelopes obtained using P1 and P2 at 2.7 and 2.0 m from the beginning of the slot during the water test

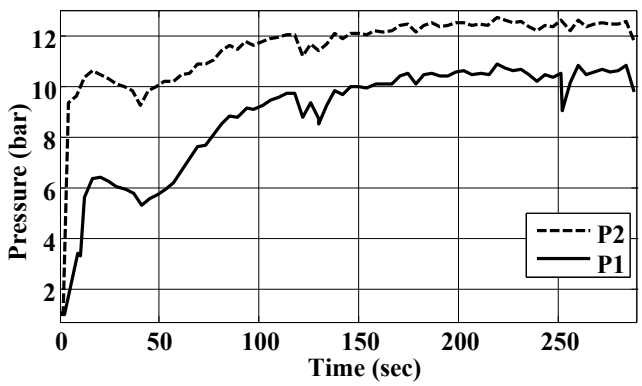

Fig. 40 The max-pressure envelopes obtained using P1 and P2 at 2.7 and 2.0 m from the beginning of the slot during the grout test

4.3 Conclusions

The general outcomes of part (c) can be summarized as follows:

- Application of low-frequency rectangular pressure impulse in the experiments using Short slot showed a substantial control of filtration as a means to improve the grout spread even in constrictions narrower than 70 μm.
- The analysis of total weight of passed grout and the CMFRs showed better control of filtration in experiments conducted at 2 s/2 s peak/rest periods using both 30 and 43 μm slots.
- The analysis of min-pressure envelopes revealed that the cycles with dominant erosion were the main reason to keep the partially plugged constrictions open for further grout spread.
- The analysis of the CMFRs showed leading filtration over the first cycle, dominating the flow rate throughout the experiment. A key factor to improve the grout spread in dynamic grouting would therefore be better control of the filtration over the first cycle.
- The study suggested that during application of rectangular pressure impulse, the greater the pressure variation the better the control of filtration and consequently the greater the grout spread.
- The study finally revealed that, in the experiments using VALS, the remaining amplitudes of the pressure impulses after 2.0 and 2.7 m (with aperture ranges of 230-70 and 230-50 μm) can be as large as 46% and 25% of the initial/applied amplitude to influence the grout spread.

5. Evaluation of the RTGC theory - Part (d)

The fundamental assumptions of the theory are constant grout-rheological properties over time, no filtration, and uniform fracture aperture. In common grouting practice, the grout-rheological properties can be assumed constant depending on the recipe and the materials used. The filtration that occurs at a fracture constriction might, however, interfere with the second assumption if the grout flow is sustained through the fracture (Eriksson and Stille 2003; Eklund and Stille 2008; Ghafar et al. 2017a). Concerning the third assumption, all the laboratory work conducted to verify the RTGC theory was done either in pipes or in parallel plates with constant apertures (Håkansson 1993; Gustafson et al. 2013). This means that the theory has not yet been sufficiently investigated in the lab in the presence of constrictions and varying apertures similar to rock fractures.

Since the physical aperture in rock fractures cannot be directly determined, using a couple of water tests, a rough estimation of the corresponding aperture is normally obtained in the form of a hydraulic aperture, b_h. This, however, is the aperture size used previously in predictions of the early stages of the development of the RTGC theory. But it is not b_h that governs the grout take in grouting operations; it is the fracture's mean physical aperture, b_{phy}. Several investigations have therefore been carried out to find the relationship between b_{phy} and b_h using the standard deviation of the physical apertures and the relative contact area of the fracture walls (Zimmerman and Bodvarsson 1996; Tsuji et al. 2012; Stille 2015). The estimated b_{phy}, which is used nowadays as the aperture in predictions using the RTGC theory, is roughly 2.0 times the size of b_h (Stille 2015). Accordingly, the main objectives in this part of the study were to answer the following research questions:

- Is it feasible to employ the RTGC theory to predict the grout spread in an artificial fracture with variable apertures?
- How good is b_h or b_{phy} employed in the RTGC theory to predict the grout propagation in an artificial fracture?

5.1 Analytical evaluation of grout propagation over time

To predict the grout propagation in VALS using the RTGC theory, the geometry, the material properties, and the applied pressure were required.

5.1.1 Geometry

In Fig. 41, the cross-section of VALS is presented with 4 m length, 0.10 m width, and descending apertures of 230-10 μm.

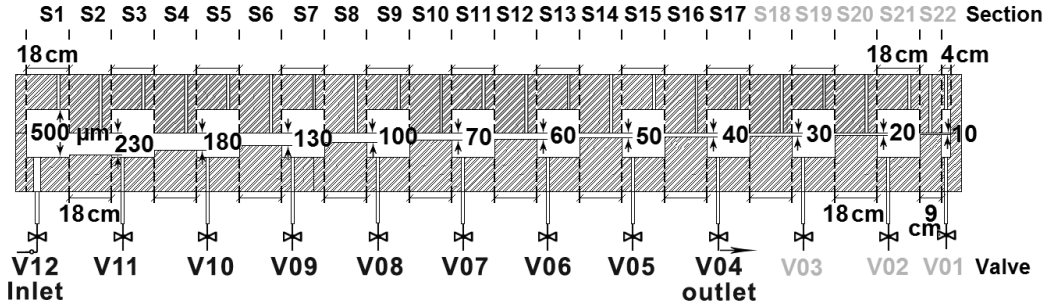

Fig. 41 Geometry and sections of varying aperture long slot (VALS)

In the set-up used, since the estimated b_{min} of the selected grouts was 40 µm, valves V12 and V04 were selected as the inlet and outlet, respectively. Therefore, only 2.88 m of VALS with eight chambers of 500 µm aperture and eight constrictions of 230-40 µm apertures (i.e. sections S1-S16) were used in the investigation. Hence, b_{phy} of VALS was determined by calculating the average of the corresponding apertures.

To back-calculate b_h, the results of two water tests conducted at 15 bar pressure were employed. The calculation was carried out based on the results of the weight-time measurements using the cubic law presented in Eq. 3.

$$Q = \frac{\rho_w . g}{12 . \mu_w} . w . {b_h}^3 . \frac{H}{L} \qquad \text{Eq. 3}$$

where Q is the volumetric flow rate, ρ_w the density of water, μ_w the dynamic viscosity of water, g the acceleration due to gravity, w the width of the slot, and H the sum of the head losses between the inlet and outlet located at distance L (Stille 2015).

5.1.2 Material properties

The properties of the selected materials (i.e. the density, ρ, the dynamic viscosity, μ, and the yield stress, τ_o) were determined using a Mud balance and a conventional rotational rheometer, a Brookfield DV-II+, respectively (Hässler 1991; Håkansson 1993).

5.1.3 Estimation of grout propagation using RTGC theory

In order to predict the grout propagation using the RTGC theory, the characteristic grouting time, t_o (i.e. the time for reaching 80% of the possible penetration length), the relative grouting time, t_D, and the relative grout penetration length, I_D, were first determined using Eqs. 4-6 (Gustafson and Stille 2005; Gustafson et al. 2013).

$$t_0 = \frac{6 . \Delta p . \mu}{{\tau_0}^2} \qquad \text{Eq. 4}$$

$$t_D = \frac{t}{t_0} \qquad \text{Eq. 5}$$

$$I_D = \frac{I}{I_{max}} \qquad \text{Eq. 6}$$

where Δp is the difference between the grouting pressure and the resisting water pressure, I the grout penetration length at time t, and I_{max} the maximum penetration length. As suggested by Hässler (1991), I_{max} was then calculated using Eq. 7.

$$I_{max} = \frac{\Delta p . b}{2 . \tau_0} \qquad \text{Eq. 7}$$

where b is the fracture aperture.

In order to calculate I versus t, the correlation between I_D and t_D was approximated for 1D (one-dimensional) flow condition using Eqs. 8, 9 (Stille et al. 2009).

$$\theta_{1D} = \frac{t_D}{2 . (0.6 + t_D)} \qquad \text{Eq. 8}$$

$$I_D = \sqrt{\theta_{1D}^2 + 4 . \theta_{1D}} - \theta_{1D} \qquad \text{Eq. 9}$$

Accordingly, I was predicted in real time during the grouting process in VALS using the flow chart presented in Fig. 42.

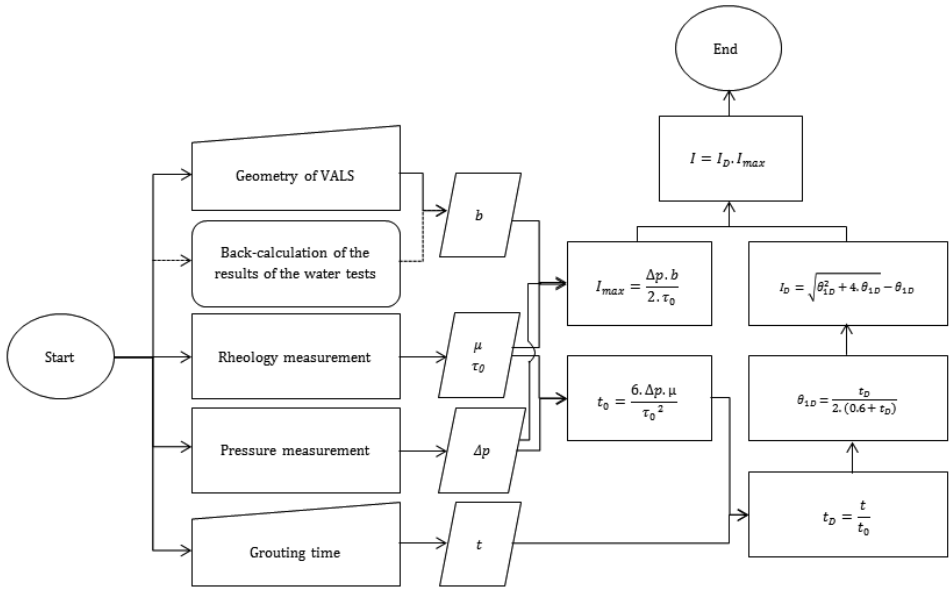

Fig. 42 Estimation of grout propagation over time using the RTGC theory

5.2 Experimental evaluation of grout propagation over time

5.2.1 Materials, mixing process, and test plan

The materials used in part (d) of the study were tap water, cement-based grout with two recipes, and two synthetic oil samples. The cement, the water-to-cement (w/c) ratio and the super-plasticizer used in both grout samples were as described earlier in part (a). However, the concentrations of the super-plasticizer were 0.5% and 0.18% in recipes R1 and R2, respectively. Finally, the oil samples were SAE20 and SAE50. The grout samples were prepared based on the same mixing process as described earlier in part (a). The experiments were all conducted at a static pressure of 15 bar, according to the test plan presented in Table 8.

Table 8 Test plan

Group	Test No.	Materials	Pressure (bar)
G1	G1-T1	Tap water	15
	G1-T2	Tap water	15
G2	G2-T1	Grout R1	15
	G2-T2	Grout R1	15
	G2-T3	Grout R2	15
	G2-T4	Grout R2	15
G3	G3-T1	Oil SAE 20	15
	G3-T2	Oil SAE 50	15

Grout R1: Cement (INJ30), W/C (0.8), i-flow1 (0.5%)
Grout R2: Cement (INJ30), W/C (0.8), i-flow1 (0.18%)

5.2.2 Test apparatus and procedure

The test apparatus used in part (d) of the study is presented in Fig. 43. All the components were the same as in the test set-up described in part (b). However, VALS was equipped with three pressure sensors P1-P3 located at 0.99, 1.71, and 2.43 m from the inlet.

In each experiment, the grout tank was first filled and pressurized. Each test was initiated by opening V12, while all valves except V04 were closed. In each test, the weight of the injected materials was registered over time. The corresponding results obtained from the water tests were used to back-calculate b_h. To monitor the grout front, the time intervals at which the pressure began to rise at each pressure sensor were plotted against the corresponding distances from the inlet. All tests were conducted in dry condition to assure that residue from the previous tests had no influence on the results.

5.3 Summary of the results and discussion

5.3.1 Material properties

The results obtained from the density and rheology measurements of the materials are summarized in Table 9.

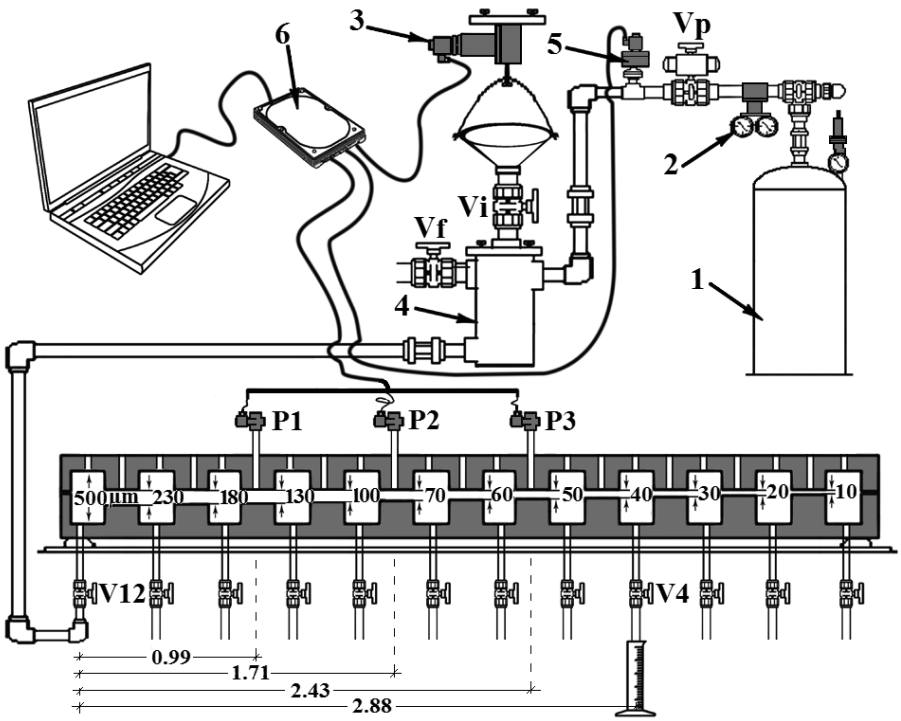

Fig. 43 Schematic view the test set-up: 1) gas tank, 2) pressure regulator, 3) load cell, 4) grout tank, 5) pressure sensor, 6) DAQ – data acquisition system

Table 9 Estimation of the material properties

Materials	ρ (kg/m^3)	μ (Pa.s)	$\tau 0$ (Pa)
Tap water	1000	1.3e-3	-
Grout R1	1610	8.3e-3	0.08
Grout R2	1600	5.70e-3	1.01
Oil SAE 20	880	142.1e-3	0.14
Oil SAE 50	950	754.6e-3	0.55

5.3.2 Hydraulic and mean physical apertures

The measurement of weight over time obtained from the water tests (G1-T1 and G1-T2) resulted in a Q of approximately 5.30e-6 m^3/sec. By substituting Q and the other known values in Eq. 3, b_h of VALS (between V12 and V04) was estimated to be 117 µm (Table 10). By calculating the average of the physical apertures of sections S1-S16, located between V12 and V04, b_{phy} of VALS was then estimated to be 304 µm. This is almost 2.6 times the size of the estimated b_h, which is in agreement with the previous findings of Tsuji et al. (2012) and Stille (2015).

Table 10 Estimation of the hydraulic aperture based on the results of the water tests

Test No.	M (kg)	ρ (kg/m^3)	V (m^3)	t (s)	$Q=V/t$ (m^3/s)	$i=H/L$ (-)	L (m)	μ (Pa.s)	g (m/s^2)	W (m)	bh (µm)
T1-G1	2.10	1000	2.1e-3	398.68	5.30e-6	150	2.88	1.3e-3	9.81	0.10	117

5.3.3 Tracking the grout front using the pressure-time measurements

The results of the pressure-time measurements obtained from the experiments conducted using Grout R1 are presented in Fig. 44 (G2-T1 left and G2-T2 right). These results, however, were only employed in this study to register the time when the grout front reached the respective location of each sensor. The time intervals for grout R1 to reach pressure sensor P1, P2, and P3 in tests G2-T1 and G2-T2 were 0.6, 5.9, 23.2 sec and 0.55, 5.1, and 20.4 sec, respectively (Fig. 44). These time intervals were subsequently plotted against the respective distances of the pressure sensors (P1-P3) from the inlet (i.e. 0.99, 1.71, and 2.43 m) to monitor the corresponding grout propagation over time (Fig. 45 left). A similar process was applied to all materials in test groups G2 and G3.

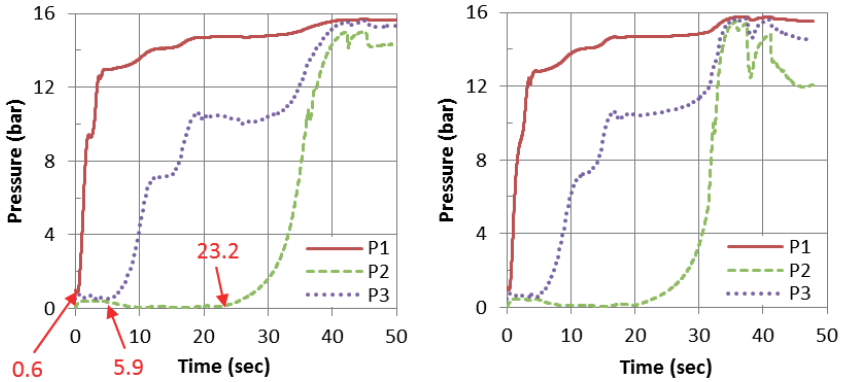

Fig. 44 Results of the pressure-time measurements in experiments conducted using Grout R1 (G2-T1 left and G2-T2 right) to monitor the grout propagation over time

5.3.4 Experimental and predicted grout propagation (Grouts R1-R2)

The experimental and the predicted penetration length over time using both b_h and b_{phy} for grouts R1 and R2 (G2-T1, G2-T2, G2-T3, and G2-T4) are presented in Fig. 45. As can be seen, the predicted results using b_h, the way that the theory was used previously in the early stages of the development, showed relatively good agreement with the experimental results for both grout samples. At the beginning of VALS, the predictions showed a slower spread (as anticipated), where the slot's physical aperture was considerably larger than b_h. The predicted spread then gradually became faster than the experimental results due to the decrease in the slot's physical apertures. Since the smaller the apertures the higher the potential for filtration, through the reduction of the apertures along VALS, the grout flow would be increasingly subject to filtration. This might also have some influence on obtaining slower experimental results than the predicted spread through reduction of the apertures. The corresponding trend was similar in the experiments with both grout samples. The results predicted using b_{phy}, the way that the theory is used nowadays to predict grout propagation in the field, however, are considerably faster than the experimental results for all the tested materials. This suggests that use of b_{phy} as discussed by Zimmerman and Bodvarsson (1996), Tsuji et al. (2012), and Stille (2015) does not always give a good approximation of the fracture apertures to use in predictions using the RTGC theory. Depending on the geometry conditions, b_h might be a better choice for this purpose. This, however, needs further investigation using different distributions of the apertures. Similar trends can be seen in the experiments with oil samples.

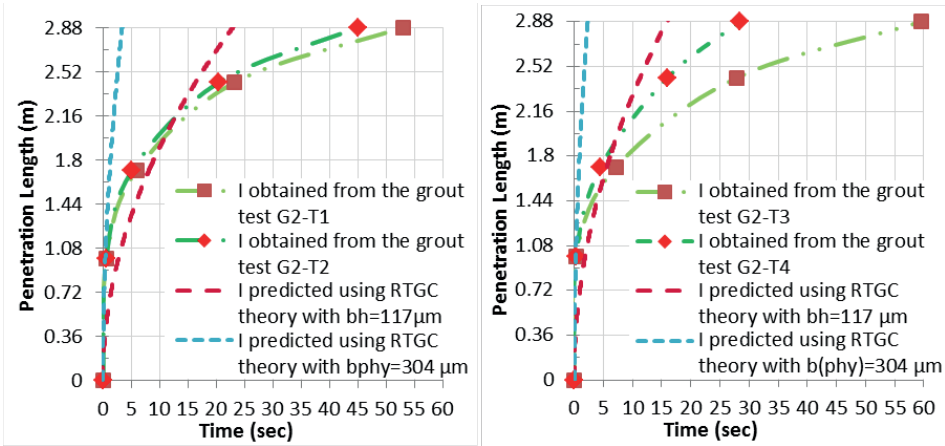

Fig. 45 Experimental and predicted grout propagation over time for grout R1 (left, G2-T1 and G2-T2) and grout R2 (right, G2-T3 and G2-T4)

5.4 Conclusions

The general outcomes of part (d) can be summarized as follows:

- The predictions of grout propagation obtained from the RTGC theory using b_h, the way that the theory was used previously in the early stages of the development, showed relatively good agreement with the experimental results for all the tested materials. However, the predictions using b_{phy}, the way that the theory is nowadays used in field applications, showed considerably faster spread than the experimental results.
- This suggests that use of b_{phy} does not always give a good approximation of the fracture apertures to employ in predictions using the RTGC theory. Depending on the geometry conditions, use of b_h might provide a more realistic prediction of the grout spread.

6. Future studies

6.1 Planned future work

Application of low-frequency rectangular pressure impulse in VALS using different pressure set-ups and materials is the next step in the current research. This project has been defined as a senior research project funded by BeFo with the aim of studying the influence of different peak/rest periods on the dissipation of the pressure impulses along an artificial fracture and eventually on grout spread.

6.2 Suggestions for future projects

To transform the existing grouting technology (using static pressure) into a more robust grouting technique with enhanced efficiency in rock grouting (using dynamic pressure), a new PhD project is proposed on application of low-frequency rectangular pressure impulse as a supplement to the current investigation. The proposed project can also provide a basis for the new generation of grouting injection pumps specified for rock grouting. The project can be outlined as lab-scale experiments, analytical and numerical studies of the method, and finally field-scale experiments in the Äspö hard rock laboratory.

In order to provide the opportunity for in-line evaluation of grout penetrability properties in rock fractures in the field, a portable version of VALS with a tubular cross-section is suggested that can be developed within the framework of a senior research project. The proposed test apparatus, which can be simply installed and used in any grouting unit, would be a huge step towards a standard test methodology to measure grout penetrability properties more realistically. The method can also be used to study the influence of aperture distribution on the prediction of grout propagation using the RTGC theory, since the test apparatus can be used with different aperture order.

7. References

Andreou, P., W. Frikha, R. Frank, J. Canou, V. Papadopoulos, and J. C. Dupla. 2008. "Experimental Study on Sand and Gravel Columns in Clay." In *Proceedings of the Institution of Civil Engineers-Ground Improvement* 161(4): 189–198. doi:10.1680/grim.2008.161.4.189.

Atkinson, R.H., and M.P. Schuller. 1993. "Evaluation of Injectable Cementitious Grouts for Repair and Retrofit of Masonry." In *Masonry: Design and Construction, Problems and Repair*. Philadelphia: ASTM International. doi:10.1520/STP19626S.

Axelsson, M., and G. Gustafson. 2007. "Grouting with High Water/solid-Ratios. Literature and Laboratory Study." Gothenburg: Chalmers University of Technology.

Axelsson, M., and G. Gustafson. 2010. "The PenetraCone, a New Robust Field Measurement Device for Determining the Penetrability of Cementitious Grouts." *Tunnelling and Underground Space Technology* 25 (1): 1–8. doi:10.1016/j.tust.2009.06.004.

Axelsson, M., G. Gustafson, and Å. Fransson. 2009. "Stop Mechanism for Cementitious Grouts at Different Water-to-Cement Ratios." *Tunnelling and Underground Space Technology* 24 (4): 390–397. doi:10.1016/j.tust.2008.11.001.

Banfill, P.F.G. 2006. "Rheology of Fresh Cement and Concrete." *Rheology Review* 2006. British Society of Rheology: 61–130. doi:10.4324/9780203473290.

Bergman, S. 1970. "Tunneltätning. Injekteringsmedelinträngning I Sand Och Smala Spalter, Byggforskningen Rapport R45." Rotobeckman AB, Stockholm.

Borgesson, L., and L. Jansson. 1990. "Grouting of Fractures Using Oscillating Pressure." In *International Conference on Mechanics of Jointed and Faulted Rock*: 875–82. Vienna, A. A. Balkeme, Rotterdam.

Draganovic, A. 2009. "Bleeding and Filtration of Cement-Based Grout." *Doctoral Thesis*, Royal Institute of Technology-KTH, Stockholm, Sweden.

Draganovic, A., and H. Stille. 2011. "Filtration and Penetrability of Cement-Based Grout: Study Performed with a Short Slot." *Tunnelling and Underground Space Technology* 26 (4): 548–59. doi:10.1016/j.tust.2011.02.007.

Draganovic, A., and H. Stille. 2014. "Filtration of Cement-Based Grouts Measured Using a Long Slot." *Tunnelling and Underground Space Technology* 43: 101–12. doi:10.1016/j.tust.2014.04.010.

Eklund, D. 2005. "Penetrability Due to Filtration Tendency of Cement Based Grouts." *Doctoral Thesis*. Royal Institute of Technology-KTH, Stockholm, Sweden.

Eklund, D., and H. Stille. 2008. "Penetrability due to Filtration Tendency of Cement-Based Grouts." *Tunnelling and Underground Space Technology* 23 (4): 389–98. doi:10.1016/j.tust.2007.06.011.

Eriksson, M., T. Dalmalm, M. Brantberger, and H. Stille. 1999. "Separations-Och Filtrerings Stabilitet Hos Cementbaserade Injekteringsmedel (Raport 3065 in Swedish)." Royal Institute of Technology-KTH, Stockholm, Sweden.

Eriksson, M., M. Friedrich, and C. Vorschulze. 2004. "Variations in the Rheology and Penetrability of Cement-Based Grouts - An Experimental Study." *Cement and Concrete Research* 34 (7): 1111–19. doi:10.1016/j.cemconres.2003.11.023.

Eriksson, M., H. Stille, and J. Andersson. 2000. "Numerical Calculations for Prediction of Grout Spread with Account for Filtration and Varying Aperture." *Tunnelling and Underground Space Technology* 15 (4): 353–64. doi:10.1016/S0886-7798(01)00004-9.

Eriksson, M, and H Stille. 2003. "A Method for Measuring and Evaluating the Penetrability

of Grouts." In *3rd International Conference on Grouting and Ground Treatment*, 1326–37. New Orleans, Louisiana, United States: ASCE. doi:10.1061/40663(2003)79.

Fransson, Å. 2008. "Grouting Design Based on Characterization of the Fractured Rock, Presentation and Demonstration of a Methodology (Technical Report R-08-127)." Swedish Nuclear Fuel and Waste Management AB (SKB), Stockholm, Sweden.

Gandais, M., and F. Delmas. 1987. "High Penetration C3S Bentonite-Cement Grouts for Finely Fissured and Porous Rock." In *International Conference on Foundations and Tunnels*: 29–33. London, UK.

Ghafar, A.N., S. Ali Akbar, M. Al-Naddaf, A. Draganovic, and S. Larsson. 2017a. "Uncertainties in Grout Penetrability Measurements ; Evaluation and Comparison of Filter Pump , Penetrability Meter and Short Slot." *Geotechnical and Geological Engineering*. Springer. doi:10.1007/s10706-017-0351-4.

Ghafar, A.N., A. Mentesidis, A. Draganovic, and S. Larsson. 2016. "An Experimental Approach to the Development of Dynamic Pressure to Improve Grout Spread." *Rock Mechanics and Rock Engineering* 49 (9). Springer: 3709–3721. doi:10.1007/s00603-016-1020-2.

Ghafar, A.N., S. Sadrizadeh, A. Draganovic, F. Johansson, U. Håkansson, and S. Larsson. 2017c. "Application of Low-Frequency Rectangular Pressure Impulse in Rock Grouting." In *Grouting 2017: Grouting, Drilling, and Verification*. *ASCE Geotechnical Special Publication 288*: 104-113. doi:10. 1061/9780784480793.010.

Ghafar, A.N., S. Sadrizadeh, K. Magakis, A. Draganovic, and S. Larsson. 2017b. "Varying Aperture Long Slot (VALS), a Method for Studying Grout Penetrability into Fractured Hard Rock." *Geotechnical Testing Journal*. ASTM. 40 (5): 871–882. doi:10.1520/GTJ20160179.

Grøv, E., and O. Woldmo. 2012. "Modern Pre-Grouting Technology in Norway." In *4th International Conference on Grouting and Deep Mixing*: 805–15. New Orleans, Louisiana, United States: ASCE. doi:10.1061/9780784412350.0064.

Gustafson, G., J. Claesson, and Å. Fransson. 2013. "Steering Parameters for Rock Grouting." *Applied Mathematics* 2013: 1–9. doi:10.1155/2013/269594.

Gustafson, G., and H. Stille. 2005. "Stop Criteria for Cement Grouting." *Felsbau: Zeitschrift Für Geomechanik Und Ingenieurgeologie Im Bauwesen Und Bergbau* 25 (3): 62–68.

Gustafson, G, and H Stille. 1996. "Prediction of Groutability from Grout Properties and Hydrogeological Data." *Tunnelling and Underground Space Technology* 11 (3): 325–332.

Hansson, P. 1995. "Filtration Stability of Cement Grouts for Injection of Concrete Structures." In *IABSE Symposiun*, 1199–1204. San Fransisco.

Hjertström, S. 2001. "Microcement-Pentration Versus Particle Size and Time Control." In 4*th Nordic Rock Grouting Symposium, SveBeFo Rapport 55*: 61-71. Stockholm, Sweden.

Houlsby, A.C. 1990. *Construction and Design of Cement Grouting: A Guide to Grouting in Rock Foundations (Vol. 67)*. John Wiley & Sons.

Håkansson, U. 1993. "Rheology of Fresh Cement-Based Grouts." *Doctoral Thesis,* Royal Institute of Technology-KTH, Stockholm, Sweden.

Hässler, L. 1991. "Grouting of Rock – Simulation and Classification." *Doctoral Thesis,* Royal Institute of Technology, Stockholm, Sweden.

Kobayashi, S., H. Stille, G. Gustafson, and B. Stille. 2008. "Real Time Grouting Control Method: Development and Application Using Äspö HRL Data." Stockholm, Sweden.

Lombardi, G. 2003. "Grouting of Rock Masses." In 3*rd International Conference on Grouting*

and Ground Treatment: 164–97. New Orleans, Louisiana, US: ASCE. doi:10.1061/40663(2003)6.

Miltiadou-Fezans, A., and T.P. Tassios. 2012. "Fluidity of Hydraulic Grouts for Masonry Strengthening." *Materials and Structures* 45 (12): 1817–1828. doi:10.1617/s11527-012-9872-8.

Mohammed, M.H., R. Pusch, and S. Knutsson. 2015. "Study of Cement-Grout Penetration into Fractures under Static and Oscillatory Conditions." *Tunnelling and Underground Space Technology* 45: 10–19. doi:10.1016/j.tust.2014.08.003.

Mohammed, M.H., R. Pusch, S. Knutsson, and G. Hellström. 2014. "Rheological Properties of Cement-Based Grouts Determined by Different Techniques." *Engineering* 6 (5): 217–29. doi:10.4236/eng.2014.65026.

Nobuto, J., M. Nishigaki, S. Mikake, S. Kobayashi, and T. Sato. 2008. "Prevention of Clogging Phenomenon with High-Grouting Pressure." *Doboku Gakkai Ronbunshuu C.* 64 (4): 813–832 (in Japanese with English abstract). doi:10.2208/jscejc.64.813.

Paillere, A.M., M. Buil, A. Miltiadou, R. Guinez, and J.J. Serrano. 1989. "Use of Silica Fume and Superplasticizers in Cement Grouts for Injection of Fine Cracks." In *3rd International Conference on the Use of Fly Ash, Silica Fume, Slag and Natural Pozzolans in Concrete*, 114:1131–58. Trondheim: SP-ACI.

Pusch, R., M. Erlström, and L. Börgesson. 1985. "Sealing of Rock Fractures A Survey of Potentially Useful Methods and Substances (Technical Report 85-17)." Swedish Nuclear Fuel and Waste Management Co (SKB), Stockholm, Sweden.

Pusch, R., S. Knutsson, G. Ramqvist, M.H. Mohammed, and A. Pourbakhtiar. 2012. "Can Sealing of Rock Hosting a Repository for Highly Radioactive Waste Be Relied on ?" *Natural Science* 4 (Special): 895–905. doi:10.4236/ns.2012.431117.

Karol, R.H. 2003. *Chemical Grouting and Soil Stabilization, Revised and Expanded*. 3rd ed. Taylor & Francis. doi:10.1201/9780203911815.

Rafi, J.Y. 2013. "Design Approaches for Grouting of Rock Fractures; Theory and Practice (BeFo Report 124)." Rock Engineering Research Foundation-BeFo, Stockholm, Sweden.

Sandberg, P. 1997. "NES-Metod För Mätning Av Injekteringsbruk Inträngningsförmåga." *Svensk Bergs- & Brukstidning, 5–6/97*.

Schwarz, L.G. 1997. *Roles of Rheology and Chemical Filtration on Injectability of Micro Fine Cement Grouts*. Northwestern University.

Stille, B., H. Stille, G. Gustafson, and S. Kobayashi. 2009. "Experience with the Real Time Grouting Control Method." *Geomechanics and Tunneling* 2: 447–59.

Stille, H. 2015. *Rock Grouting-Theories and Applications*. Rock Engineering Research Foundation-BeFo, Stockholm, Sweden.

Stille, H., G. Gustafson, and L. Hässler. 2012. "Application of New Theories and Technology for Grouting of Dams and Foundations on Rock." *Geotechnical and Geological Engineering* 30 (3): 603–24. doi:10.1007/s10706-012-9512-7.

Tsuji, M., M. Holmberg, B. Stille, J.Y. Rafi, and H. Stille. 2012. "Optimization of the Grouting Procedure with RTGC Method. Data from a Trail Grouting at City Line Project in Stockholm." Stockholm, Sweden.

Wakita, S., K. Aoki, Y. Mito, Y. Kurokawa, T. Yamamoto, and K. Date. 2003. "Development of Dynamic Grouting Technique for the Improvement of Low-Permeable Rock Masses." In 1st *Kyoto International Symposium on Underground Environment*, 341–48. doi:10.1201/NOE9058095565.ch44.

Warner, J. 2004. *Practical Handbook of Grouting: Soil, Rock and Structures*. John Wiley & Sons.

Weideborg, M., T. Källqvist, K.E. Ødegård, L.E. Sverdrup, and E.A. Vik. 2001. "Environmental Risk Assessment of Acrylamide and Methylolacrylamide from a Grouting Agent Used in the Tunnel Construction of Romeriksporten, Norway." *Water Research* 35 (11): 2645–52. doi:10.1016/S0043-1354(00)00550-9.

Widmann, R. 1996. "International Society for Rock Mechanics Commission on Rock Grouting." *Rock Mechanics and Mining Sciences & Geomechanics Abstracts* 33 (8): 803–847. doi:10.1016/S0148-9062(96)00015-0.

Zebovitz, S., R.J. Krizek, and D.K. Atmatzidis. 1989. "Injection of Fine Sands with Very Fine Cement Grout." *Geotechnical Engineering* 115 (12): 1717–33. doi:10.1061/(ASCE)0733-9410(1989)115:12(1717).

Zimmerman, R.W., and G.S. Bodvarsson. 1996. "Hydraulic Conductivity of Rock Fractures." *Transport in Porous Media* 23: 1–30.

BeFo

Box 5501
SE-114 85 Stockholm

info@befoonline.org • www.befoonline.org
Visiting address: Storgatan 19, Stockholm

ISSN 1104-1773